Trawling-induced resuspension and dispersal of muddy sediments and dissolved elements in the Gulf of Lion (NW Mediterranean)

Xavier Durrieu de Madron, B Ferre, G Le Corre, Christian Grenz, P Conan, Mireille Pujo-Pay, R Buscail, O Bodiot

Continental Shelf Research
December 2005; 25(19-20) : 2387-2409
http://dx.doi.org/10.1016/j.csr.2005.08.002

Trawling-induced resuspension and dispersal of muddy sediments and dissolved elements in the Gulf of Lion (NW Mediterranean)

X. Durrieu de Madron[a*], B. Ferré[a], G. Le Corre[b], C. Grenz[c], P. Conan[d], M. Pujo-Pay[d], R. Buscail[a] and O. Bodiot[a]

[a]CEFREM, UMR 5110, CNRS—Université de Perpignan, 52 Avenue de Villeneuve, 66860 Perpignan Cedex, France
[b]Laboratoire Ressources Halieutiques, IFREMER DRV/RH, Bd Jean Monnet, BP 171, 34203 Sète Cedex, France
[c]Station Marine Endoume, UMR 6535 CNRS—LOB, Rue de la Batterie des Lions, 13007 Marseille, France
[d]Observatoire Océanologique de Banyuls, Laboratoire d'Océanographie Biologique, UMR 7621, CNRS-UPMC, 66651 Banyuls-sur-Mer Cedex, France

*: Corresponding author : Fax: +33 4 6866 2096. demadron@univ-perp.fr

Abstract: A dedicated trawling experiment was performed at three sites on the Gulf of Lion continental shelf, with the aim of assessing the resuspension of particulate and dissolved matter triggered by different types of trawls on muddy sediments. The different configurations were: (i) bottom trawl, with bobbin for ground rope (Rockhopper): (ii) bottom trawl, without bobbin (Medits); and (iii) pelagic trawl, towed at 1 and 10 m above the seabed.
The plumes of resuspended sediment were measured using the acoustic backscattered intensity, from a towed ADCP. Concomitant profiles of particle size-distribution, light transmission and water samples were collected, outside and inside the plumes. The analysis of the data enabled derivation of the major physical and chemical characteristics of the plumes generated by the trawls; likewise, and to quantify the resuspension fluxes of sediment, particulate (PN, POC) and dissolved (nutrients) elements. The residence time and dispersal of the plumes were monitored and modelled, considering the settling velocity of the particulate matter and the near-bottom turbulence.
The results indicate that the bottom trawls produce significant resuspension, whilst the near-bottom and mid-water pelagic trawls have no impact upon the sediment. The sediment clouds at several hundreds metres astern of the bottom trawls are 3–6 m high and 70–200 m wide; they were generated both by the otter doors and the net. The average suspended sediment concentrations measured in the plumes reach 50 mg l−1. Resuspension fluxes of sediment along the path of the trawls range from 190 g m−2 s−1, for the coarsest sediment (clayey silt) to 800 g m−2 s−1 for the finest sediment (silty clay). Whilst the resuspended loads of dissolved elements (nutrients) within the plume segment suggest a release of porewater, present at least in the first few centimetres of sediment, the particulate matter load only resulted from the resuspension of less than 1 mm thickness of the sediment bed. This discrepancy shows that a very small fraction of the sediment ploughed by the trawl is effectively injected into the water column.
The monitoring of the settling of the plumes indicates a rapid decay of the sediment load, during the first hour after its generation. Some of the sediment (about 10–15% of the initial load) remains in suspension; this is due, probably, to the near-bottom turbulence that prevents the redeposition of the fine particles and aggregates. Lateral spreading of the plume is strongly dependent upon the variability of horizontal currents.

Keywords: Coastal fisheries; Bottom trawling; Cohesive sediments; Sediment resuspension; Suspended particulate matter; Gulf of Lion; Northwestern Mediterranean Sea

INTRODUCTION

Morgan and Chuenpagdee (2003) considered, in a recent survey, that mobile demersal fishing gears (trawls, dredges, gillnets) have a relatively high ecological impact, while midwater fishing gears have a low impact on the marine environment. Demersal fishing gears are used to capture species that live or feed in benthic habitats, and thus are designed to maximise their contact with the seabed. They have marked environmental impact in terms of ploughing of the substrate, resuspension of sediment, chemical exchanges between sediments and water, and alteration of benthic habitats (Riemann and Hoffman, 1991; Jones, 1992, Pilskaln *et al.*, 1998; Watling and Norse, 1998; Rester, 2000). Various studies, based on mapping of trawl tracks or fishing activity records, indicate that commercial trawling can resuspend sediments over large areas of continental shelves and that some intensively fished regions can be swept by trawls several times each year (Churchill, 1989 and the references therein; Watling and Norse, 1998). The resuspension of muddy sediment by trawl gears produces highly turbid plumes of suspended particles with concentrations up to several hundreds mg l^{-1} near the seabed (Schoellhamer, 1996). As a consequence of both the intensity of the fishing activity and effect of trawl on sediment resuspension, Churchill (1989) estimated from a simple model that trawling on the Middle Atlantic Bight can be a significant source of suspended sediment over the outer shelf, where the wave-induced resuspension is weak. In the Kattegat Sea, Floderus and Pihl (1990) estimated that bottom trawling deeper than 10-20 m shortened significantly the recurrence time of sediment resuspension induced by wind waves. Peng and Broecker (1984) questioned the impact of trawling activities on the disruption of benthic communities and the subsequent reduction of the recycling of freshly deposited organic matter in the shelf sediments. In this scenario, the extra carbon incorporated into sediments could contribute to the sink of anthropogenic carbon.

The assessment of the trawling disturbance on the coastal environment is a complex task because the magnitude of sediment resuspension by trawls is affected by various factors (e.g., physical dimensions and type of gear, the nature of the substratum). Very little work has been done to date on the direct characterisation of the turbid plume dimensions. Main and Sangster (1981) measured sediment clouds produced by trawls on fine sand bottom of a few meters high and wide. Sediment clouds produced on muddy bottom are believed to have a larger size, up to 10 m high and 50 m wide astern of trawls (Churchill, 1989 and the references therein). Furthermore, the resuspension fluxes of particulate and dissolved elements and their fate are essentially unknown. A few observations suggested that some of the muddy sediment resuspended by trawls could remain in suspension for long period of time (up to 48 hours) and contribute to the maintenance of the bottom nepheloid layer (Schoellhamer, 1996; Pilskaln *et al*., 1998; Palanques *et al*., 2001). Churchill (1998) stated that «From a sediment dynamics viewpoint, the most fundamental issues requiring study are the effects of trawling on suspended sediment load and sediment transport. Quantifying these effects requires determining the rate at which trawls resuspend sediment (i.e., the mass of sediment put into suspension per unit track length), the height of the sediment plumes generated by trawling and the time required for these to settle. Investigating the effects of trawling on nutrient supply and on the resulting biological response will require still more involved techniques».

The present study aims to perform a comparative study of the impact of different types of trawls and substrates on the resuspension of particulate and dissolved elements and their subsequent dispersal or redeposition. This work was performed within the framework of the European INTERPOL (Impact of Natural and Trawling Events on the Resuspension and fate of POLlutants) project, and the field experiment was conducted on the Gulf of Lion continental shelf (NW Mediterranean).

Given that sediments deeper than 30 m are essentially composed of clays and silts (Durrieu de Madron *et al.*, 2000) and trawling activity is banned within a 3-mille band along the coast, this study was restricted to the impact of trawls on more or less muddy environments. Otter trawls are the most common bottom gear used by commercial fishermen in the Gulf of Lion, yet pelagic trawls are sometimes used very near the seabed to catch demersal fishes. Four trawl configurations were selected to span the largest range of potential impact on the sediment: (1) otter trawl with bobbins (Rockhopper trawl), (2) bottom trawl with a tickler chain (Medits trawl), (3) near-bottom pelagic trawl (< 1 m above the bottom), (4) mid-water pelagic trawl (*ca*. 10 m above the bottom). We assessed the resuspension triggered by these trawl configurations on three different sites with clayey silt or silty clay sediments. We measured the geometry of the turbid plumes and quantified the resuspension fluxes of particulate matter and dissolved elements (nutrients). Finally, we characterised the dispersal and settling of sediment clouds for two different hydrodynamic conditions and sediment types.

2. MATERIAL AND METHODS

2.1 Technical description of gears

A trawl net can be defined as a towed net consisting of a cone-shaped body, closed by a bag or codend and extended at the opening by wings (Fig. 1). It can be towed by one or two boats and, according to the type, is used on the bottom or in the midwater (pelagic) (Nedelec and Prado, 1990).

Otter trawls have two heavy doors, attached to the towing warps, which are towed at an oblique angle across the seabed and control the lateral opening at the mouth of the net

(Fig. 1a). The furrow imprinted by doors in the sediment along their tow path depends on their weight and the angle of attack; they are typically about 0.2 to 2 m meter wide and up to 0.3 m deep (Jones, 1992 and the references therein). The groundrope at the lower edge of the net opening and the codend also contribute to the resuspension (Watling and Norse, 1998). The GOC 73 (Grande Ouverture verticale à ailes Courtes), used in this study, is an otter trawl designed for scientific fishing experiments. The characteristics of this gear make it usable over the depth range and in the various conditions encountered in the whole survey area (Fiorentini *et al.*, 1996; Fiorentini *et al.*, 1999). The groundrope of the GOC 73 trawl is usually ballasted with a tickler chain in order to penetrate the upper layers of the sediment. This configuration is used for the Mediterranean International Trawls Surveys (Medits) and will later on be referred as "Medits trawl". The GOC 73 groundrope can also be fitted with large rubber disks or bobbins (Rockhopper). Although this additional gear device is generally used over rocky substrata, it has the highest potential for excavating sediment off the seabed, when a transverse line blocks the bobbins. This second configuration will later on be referred as "Rockhopper trawl". Once, we had the opportunity to monitor the resuspension generated by a professional trawler, whose gear and operating conditions slightly differ with the Medits trawl (heavier otter doors, higher trawling speed). This configuration will later on be referred as "Professional trawl". Their characteristics are summarized in Table 1.

The doors of pelagic trawls (Fig. 1b), when towed very near the seabed, generally stay away from it while the weights spaced along the footrope - or even the footrope – skims off the surface sediment. The pelagic trawl used in this study is a PTGM 158 (Pélagique Très Grande Maille), whose characteristics are summarised in Table 1.

Autonomous acoustic sensors (Scanmar instruments) mounted on the trawl provided real time information on its geometry during hauls. Parameters measured on the gear were: distance

between trawl doors (door spread), horizontal opening of wing tips (wingspread), vertical opening of the net, altitude of groundrope). These measurements permitted us identification of instances when the gear was not fully spread or was not on the bottom for a substantial part of the haul.

2.2 Sampling strategy

The experiment was conducted on the Gulf of Lion continental shelf in the Summer of 2002 on the R/Vs L'Europe and Thetys II. Two sites with clayey silt at 30 and 60 m bottom depth and one site with silty clay sediments at 90 m bottom depth were sampled (Fig. 2 and Table 2). The R/V L'Europe performed the trawling work, and logged the trawl geometry and ship speed. Measurements combining water sample collection for sedimentological and geochemical analysis with hydrological and hydrodynamical measurements were collected with two instrument packages towed from a second vessel, the R/V Tethys II (Fig. 3). Hydrological parameters of the water column were measured with a probe including CTD and optical sensors (transmissometer and fluorometer). On top of the probe, a rosette with 12 litres bottles and an *in situ* laser particle sizer were used to sample water at given depths and describe the spatial and temporal variation of particle size spectra. Additionally, a downward-looking 300 KHz ADCP was towed above the seabed to provide profiles of acoustic backscattering intensity and currents. A 150 KHz ADCP mounted on the hull of the ship also provided real-time currents. Sediment samples were taken at each site with a multiple corer for sedimentological and geochemical analysis.

2.3 Description of instruments and analysis techniques

Hydrological parameters

Conductivity, temperature, and pressure data were measured between the surface and the bottom with a SeaBird 9/11 CTD probe. A Benthos altimeter allowed to profile down to few tens of centimetres above the seabed and to precisely control the altitude of the water sampling.

Sediment cores

Sediment samples were obtained with a sediment multicorer Bowers & Connelly Mark VI using Perspex cores (internal diamater: 15 cm, length: 50 cm) sampling approximately 30 cm of sediment.

Optical measurements

A C-star transmissometer mounted on the CTD probe measured the transmitted light intensity (T in percent) along a fixed optical path (L = 0.25 m). The attenuation coefficient (c in m^{-1}) due to absorption and diffusion by both water and suspended particles, was derived from the transmission with the equation:

$$c = - (1/L) \, Ln \, (T)$$

Water samples were filtered up to filter saturation on pre-weighed Nuclepore filters of 0.4 µm pore size. Their solid residue weights yielded suspended sediment concentration (SSC). Duplicates were made for each water samples and divergent values (difference > 20%) were discarded. We derived a linear relation between the SSC (expressed in mg l^{-1}) and the attenuation coefficient:

$$SSC = 1.55 \, c - 0.52 \qquad (r^2 = 0.94, \, n = 40)$$

Size distributions of suspended particles outside and inside the sediment plume were measured *in situ* with a Sequoia LISST-100 laser particle sizer. This device calculated from light scattering measurements the size distribution on 32 log-spaced size classes between 1.2 and 250 µm with a sampling rate of 1 second (Agrawal and Pottsmith, 2000). The instrument was also used in laboratory to measure the grain size distribution of sonicated samples of sediment and suspended matter collected on filters.

Acoustic measurements

The towed RDI broadband 300 KHz ADCP had four acoustic transducers directed downward at 20° from vertical. It measured velocity and backscattered acoustic intensity parallel to the four acoustic beams. Using the internal compass and the tilt-meters measurements as well as the bin mapping procedure, the beams' coordinates were converted into an orthogonal earth coordinate system. Bottom tracking was used to determine the absolute water velocities within the profiling range. The echo return was sampled over 30 depth cells; the cell size was 0.2 m (shallow water mode). Due to the near bottom corruption of echo return between the main and the side lobes, the valid profiling range extended from 5-6 m a.b (meters above bottom) to 0.4 m a.b. Each ping was recorded, so the sampling rate was about 6 s.

SSC were derived from backscattered acoustic intensity with the commercial Sediview software (Land and Bray, 2000), that used the sonar equation:

$$EL = SL - 2TL + TS$$

where EL and SL are the echo and source levels respectively (in dB). TL is the transmission loss and is equal to $20 \log_{10} (R) + (\alpha_w+\alpha_s)R$, where α_w and α_s are the absorption coefficients by water and sediment respectively and R is the distance from the transducer to the depth cell. TS is the target strength and is related to the mean acoustic cross-section of the scatterers $s = Ns_s$, where N is the particle density and s_s is the individual acoustic cross-section, within an

insonified volume V. If SSC (in kg m^{-3}) is N?$_s$?$_s$, where ?$_s$ is the density and ?$_s$ is the volume, TS is equal to 10 $\log_{10}$ (SSC s_s / ?$_s$?$_s$) + 10 log (V).

The sonar equation then reads :

$$EL = SL - 40\log_{10}(R) - 2R(a_w + a_s) + 10\log_{10}(SSCs_s / r_s u_s) + 10\log_{10}(V)$$

Defining the relative backscatter intensity, measured by the ADCP and corrected from beam spherical spreading, as

$$N(R) = EL - SL + 40\log_{10}(R)$$

the SSC can be expressed as

$$10\log_{10}(SSC) = N(R) + 2R(a_w + a_s) - 10\log_{10}(s_s / r_s u_s) - 10\log_{10}(V)$$

or equivalently

$$10\log_{10}(SSC) = \left[N(R) + 2R(a_w + a_s) + Ks\right] / S$$

where $Ks = -10\log_{10}(s_s / r_s u_s) - 10\log_{10}(V)$ and $S = 10$.

Theoretically, S has a value of 10, but it is allowed to vary in the Sediview method in order to fit the backscattered intensity with the measured SSC. The calibration constants S and K_S were determined empirically for each specific experiment by fitting the acoustic-derived SSC profiles with simultaneous water samples and light transmission SSC profiles (Fig. 4). Mean values of temperature, salinity and calibration constants for each site are presented in Table 2.

Particulate nitrogen and organic carbon

Particulate nitrogen (PN) and particulate organic carbon (POC) concentrations in water samples were measured by filtration on pre-combusted (4h, 450°C) Whatman GF/F filters (pore size 0.7 µm) and by combustion of the latter filters in a Leco CN 2000 analyzer after acidification by HCl 2N to remove carbonates. Duplicate water samples were analyzed in

order to eliminate spurious measurements. The accuracy of the measurements was ±2%. Likewise, PN and POC concentrations in the upper 15 cm of the sediment were measured on subsamples of 1 cm from sediment cores.

Good relationships were derived between PN and POC concentrations and SSC (all expressed in mg l^{-1} or g m^{-3}) in the bottom water layer:

$$PN = 8.1 \times 10^{-3} SSC^{0.47} \qquad (r^2 = 0.72, n = 40)$$

$$POC = 5.7 \times 10^{-2} SSC^{0.43} \qquad (r^2 = 0.70, n = 40)$$

Inorganic nutrients

Samples for inorganic nutrients were immediately filtered on board through pre-combusted (24h, 450°C) glass fibre Whatman GF/F filters (pore size 0.7 µm) under gentle vacuum (200 mm Hg) to avoid cell breakage. All determinations were made in duplicate. For ammonia, reagents were immediately added and measurements were made manually (Koroleff, 1969). Standard error was 0.02 µM. Samples for nitrate (NO_3), nitrite (NO_2), phosphate (PO_4) and silicate ($Si(OH)_4$) determinations were immediately frozen (~20°C) in polyethylene vials and analysed after the end of the cruise. Samples were then rapidly thawed and analysed according to classical methods (Mullin and Riley, 1955; Murphy and Rilet, 1962; Wood *et al*., 1967) using the automated colorimetric techniques on a auto-analyser (Tréguer and Le Corre, 1975). Standard errors were 0.1 µM, 0.02 µM, 0.02 and 0.1 µM for NO_3, NO_2, PO_4 and $Si(OH)_4$ respectively.

Nutrient profiles in the sediment were determined on 6 replicate subcores (internal diameter 2.6 cm). These subcores were sliced in 0.4-cm intervals in the upper 2 cm, in 1-cm intervals from 2 to 4 cm, and in 2-cm intervals down to 10 cm. Interstitial water was extracted by centrifugation (4500g, 20 min.) and supernatant was carefully removed, diluted with artificial

seawater and further analysed following the same standard procedure as for overlying water samples.

Dissolved Organic Matter

All determinations were made in duplicate. Samples for Dissolved Organic Nitrogen and Phosphorus (DON & DOP) were filtered through pre-combusted glass fiber Whatman GF/F filters and directly collected in precalcinated pyrex bottles and immedialtly frozen on board (-20°C) until analyses. DON and DOP were then simultaneously determined by wet oxidation procedure (Pujo-Pay and Raimbault 1994). DON (±0.1 µmol l^{-1}) and DOP (±0.02 µmol l^{-1}) concentrations were determined from oxidation (30 min, 120°C) of the filtered samples corrected for their mineral concentrations (NO_3, NO_2 and NH_4 for DON, PO_4 for DOP).

For Dissolved Organic Carbon (DOC), water samples were also filtered through pre-combusted glass fiber Whatman GF/F filters and stored in precombusted glass tubes closed with a screw cap and a teflon liner. Each tube was poisoned with mercury chloride (5 mg l^{-1}) and stored at room temperature until analysis. DOC concentrations were determined using a High Temperature Catalytic Oxidation (HTCO) technique with a Shimadzu TOC V analyzer (Cauwet, 1994).

2.4 Characterisation of turbid plumes generated by trawls

This part of the experiment consisted of profiling particle size, light transmission, acoustic backscattering intensity, currents and water samples inside and outside the sediment plume. A profile was collected about one hour before the passage of the trawl. The path of the trawler was directed according to the near bottom currents (about few cm s^{-1}), measured at the beginning of the experiment, in order to position the second ship about 100-200 m downstream of the coming sediment plume. Moreover, the ship was located at mid course of

the haul that was about 4-5 km long. Immediately after the passage of the trawl, the CTD/rosette was lowered at 1 m a.b. and the ADCP at 5-6 m a.b., and the ship entirely transected the plume quasi-perpendicularly to the trawler's path at a speed of about 1 knot (~ 0.5 m s^{-1}). The light transmission sensor monitored in real-time when the CTD/rosette package entered the plume which occurred between 5 and 20 minutes following the passage of the trawl. Over this time period, the instrument packages were located at a distance of between 500 and 2000 m astern of the trawl. The CTD/rosette package was then profiled in a yo-yo mode within ten meters above the seabed until the end of the plume was reached (Fig. 3). Water samples were taken at 5 levels within the plume during one the downcasts. At the same time, the ADCP package that flew at a constant distance over the seabed provided a complete description of a plume segment. The obvious drawbacks of this strategy are: (i) it catches the sediment plume at some distance from the trawl and (ii) it mixes space and time during the crossing of the plume segment that lasted between 3 and 15 minutes.

On one occasion, the ADCP was towed about 30 m above the seabed (using the standard profiling mode with a cell size of 1 m) along the path of the trawl, between the stern of the trawler and about 200 m behind the codend. It permitted us to follow the short-term evolution of the height of the plume.

2.5 Quantification of the resuspension fluxes

Resuspension fluxes (F, mass of dissolved or particulate element put into suspension per unit area and unit time) were calculated for each transect as the ratio of the excess mass of a given element within the segment of the plume (Q in g) by the surface area of bottom sediment scraped by the trawl per second (A in m^2) (Fig. 5). From the observations of plume dispersal, we estimated that the lateral spreading of the plume during its crossing represented less than 10% of its initial width. A geometrical correction was included to take into account any

departure of the transect's direction from the perpendicular to the path of the trawl that formed an angle j. The equation for the resuspension flux estimate reads:

$$F = Q \cos(j) / A \Delta t$$

The surface A was estimated from the sum of the widths of the groundrope (W_{GR}) given by the horizontal opening of wingtips and of the furrows of the otter doors (W_{OD}) multiplied by the distance travelled by the trawl per unit time ($l = V_T \Delta t$) where V_T (in m s^{-1}) is the speed of the trawler and Δt is equal to one second (Fig. 5). With a door's length of 2 m and an attack angle of 30°, the width of each furrow was estimated to 1 m.

$$A = [W_{GR} + 2\ W_{OD}]\ \ l$$

The geometry and size of the plume were revealed using SSC derived from acoustic measurements $C(x,z)$ after removing the background (outside the plume) SSC profile $C_0(z)$. Due to the near bottom corruption of echo return between the main and the side lobes, SSC in the 0.4 m layer above the seabed was not measured. To take into account this layer where SSC is high, an extrapolation is made and SSC is calculated by fitting a power law on the three bottommost measured concentrations (i.e. between 0.4 and 0.8 m a.b.). The integration of the excess SSC over the volume of the sampled box (of length L, height H and width l, Fig. 5) yielded the excess sediment mass. Similarly, resuspension fluxes of particulate total nitrogen (PN) and particulate organic carbon (POC) were computed considering PN and POC concentrations (in g m^{-3}) inferred from SSC measurements. Given that the plume segment is homogeneous along the trawl's path, the equation for the excess mass of particulate matter within the segment (Q_p) reads:

$$Q = \sum_0^L \sum_0^H \left[C(x,z) - C_0(z) \right] \Delta x\ \Delta z\ \ l \qquad \text{where } x \in [0, L] \text{ and } z \in [0, H]$$

Since the plumes were sampled with some delay, the calculated resuspension fluxes should be considered as minimum values.

Concentration profiles of nutrients, collected in the central part of the plume, were insufficient to correctly map the distribution of these dissolved elements within the entire plume and prevented a correct quantification of the nutrient mass. Nonetheless, a crude and conservative estimate was done by calculating the excess mass of nutrient (in mol) contained within a fraction of the box volume. This volume had a height H and a bottom surface area A equal to that scraped by the trawl per second. The equation for the resuspension flux of dissolved elements (Q_d in mol m^{-2} s^{-1}) reads:

$$Q = A\sum_{0}^{H}\left[C(z) - C_0(z)\right]\Delta z$$

2.5 Quantification of the equivalent sediment thickness

We estimated the equivalent sediment thickness as the layer of sediment containing as much suspended sediment, particulate or dissolved elements as the excess loads found within the plume segment. The sediment thickness, h, is embedded, as an integration limit, within the equations:

$$Q = A\sum_{0}^{h}\left[r_w f(z) + r_s\left(1 - f(z)\right)\right]\Delta z \qquad \text{for bulk sediment}$$

$$Q = A\sum_{0}^{h}\left[C_s(z)\left(1 - f(z)\right)\right]\Delta z \qquad \text{for particulate elements (}PN\text{, }POC\text{)}$$

$$Q = A\sum_{0}^{h}\left[C_s(z) f(z)\right]\Delta z \qquad \text{for dissolved elements (nutrients)}$$

where Q_p and Q_d are the excess masses of a particulate or dissolved element in the plume, A the trawled surface area per second, r_s the density of mineral grain (2.64 g cm^{-3}), r_w the density of seawater (1.03 g cm^{-3}) and $f(z)$ the porosity profile. $C_s(z)$ represents the dry weight

concentrations for particulate elements or the porewater concentrations for dissolved elements.

2.6 Dispersal and settling of turbid plumes

The temporal changes of the geometrical characteristics of the sediment plume and its load were measured with the ADCP towed near the seabed. Two different strategies were used. In the first case, the sediment plume properties were determined by measuring acoustic backscattering intensity across a plume segment at various times after its generation by a trawl. Following the plume segment was a tricky task that was accomplished by using shipboard velocity profile data obtained with the hull-mounted ADCP. In the second case, four successive and parallel hauls about 200 m apart were performed perpendicularly to the bottom current. A transect starting from the most recent line crossed the different plumes. If the plumes were initially identical, this simple procedure provided the properties of a sediment plume with increasing lifetimes.

2.7 Numerical simulation of the plume deposition

An analytical approach was used to simulate the deposition of the suspended sediment, in order to estimate the amount of sediment that settled during the early stage of the sediment plume redeposition, which was not observed. Prandle (1997) derived an expression for the time sequence of sediment deposition as a function of settling velocity W_s, vertical dispersion coefficient E and water depth D. In this 1–DV approximation, neither horizontal advection nor dispersion is considered and E is assumed to remain constant both temporally and vertically.

Given an initial amount of suspended sediment M_0, and for $E/W_sD < 1$, the mass of sediment remaining in suspension takes the form :

$$M(t) = M_0 e^{-at}$$

where the exponential decay constant $a = 0.693 \times (W_s^2/E)$. The expression was fitted to the excess load of the plume segment measured at various stages of its deposition, which led to the estimate of M_0 and (W_s^2/E). Subsequently, a characteristic settling velocity W_s could be inferred using an independent estimate of the ambient vertical dispersion coefficient E, which was derived from the local Richardson number ($Ri = \frac{(g/r)\,\partial r/\partial z}{(\partial u/\partial z)^2}$) determined from the CTD and the ADCP profiles:

$$K_z = 1.67 \times 10^{-3} \left(1 + \frac{10}{3} Ri\right)^{-3/2}$$

where ρ is the density and g the gravitational acceleration. The density profile was derived from the observed temperature and salinity profiles. Likewise, the current profile was derived from the observed mean current profile measured with the towed and shipborne ADCPs.

3. RESULTS

3.1 Pre-trawling sediment and water column characteristics

Surficial (0-10 cm) sediments at CS60 site are characterised by POC content between 1 and 1.2% and PN contents between 0.08 and 0.1% (Table 2). The finer sediments at SC90 site are lower in POC (0.75-1%) and PN (0.05-0.06%) (Table 2). The mean POC/PN ratio of 15 corresponds to a typical degraded organic matter of continental shelf (Buscail *et al.*, 1995).

Pore water nutrients profiles in the ten first centimetres of sediment at CS60 and SC90 sites are similar to those observed previously at nearby stations in the Gulf of Lion (Helder, 1989; Blackburn, 1991, 1993; Denis and Grenz, 2003). Profiles at CS60 show steep gradients with concentrations ranging from 4 to 130 µM, 14 to 80 µM, 4.5 to 8.7 µM, and 50 to 160 µM in

NO_3+NO_2, NH_4, PO_4, and $Si(OH)_4$ respectively (Table 2). Like for particulate organic matter, nutrients concentrations are lower at SC90 site (Table 2).

Concentrations of particulate elements and nutrients in the sediment are higher than the concentrations in the overlying water column. During the summer sampling period, a strong thermocline and a halocline were situated at around 20 m depth at all stations (Fig. 6a). A two-layer system was also observed for SSC (Fig. 6b) and nutrients (Fig. 6c), but with a thicker upper layer. The upper layer was depleted in particles and nutrients expect for silicate (~ 0.5 to 20 µM). Nitracline and silicline were associated to a peak in SSC, fluorescence and nitrite between 40 and 50 m at CS60 site (Fig. 6) and between 35 and 80 for SC90 sites. Some traces of phosphate persist in the upper layer, but phosphocline is located 10 to 20 m deeper than nitracline and silicline. Ammonium concentration was close to the detection limit of classical methods (previously observed by Diaz *et al.*, 2000), so ammonium was not shown in Fig. 6. The increase of SSC within the bottom 15 m is typical of the bottom nepheloid layer that is systematically observed all the year over the whole shelf (Durrieu de Madron and Panouse, 1996). The POC and PN concentrations within that layer were about 0.07 and 0.01 mg l^{-1}, respectively. Fluctuations of particulate and dissolved matter concentrations in the bottom water layer, independent of resuspension, were estimated from repeated casts at the same station within a period of several hours. The results indicated that particulate matter concentrations "naturally" varied by ±50%, whereas dissolved elements concentrations varied by less than 5%.

3.2 Visualisation of turbid plumes

One direct output of the experiment was the absence of sediment plumes for pelagic trawls towed at 10 or 1 m above the bottom. Only bottom trawls generated plumes that were visible (Fig. 7). On one occasion, when the trawl did not work properly (weak contact with seabed as

suggested by the low tension on the towing warps), one could clearly distinguish three individual plumes created by the otter doors and the groundrope of the net (Fig. 7a). In normal conditions, one generally observed one single plume (Fig. 7b). Within a period of 30 minutes after its generation, plumes were up to 5.5 m high and 190 m wide (Table 3). The thickness and width of the plumes generated on the coarsest sediment (CS30 site) were significantly smaller than those observed on deeper and finer sediments (CS60 and SC90 sites). The measurements taken while towing the ADCP over the trawl revealed that the height of the plume was about 4-5 m immediately astern of the trawl. This result and those of the different transects suggest that the thickness of the sediment cloud remains uniform during the first 30 minutes after its generation.

Profiles performed outside the plume showed SSC of few mg l^{1} in the bottom layer. SSC significantly increased inside the plume and exhibited maximum measured concentrations between 15 and 70 mg l^{1} at 0.4 m a.b. (Fig. 8). Average excess concentrations in plumes range between 10 and 50 mg l^{-1}. Profiles did not show major differences between the different types of trawl, except for the site with the finest sediment where maximum concentrations for the Medits trawl were 50 % higher than that for the Rockhopper trawl (SC90, Fig. 8c). However, it is worthwhile to note that the former plume was sampled much earlier (time delay of 3 minutes) than the latter (time delay of 15 minutes) (Table 3).

3.3 Resuspension fluxes

Resuspension fluxes of sediment estimated for the different types of trawls and experimental sites are summarised in Table 3. As already shown, the sediment loads within plumes are strongly dependent on the delay between the start of measurements in the plume and its generation. As larger delays imply lower fluxes, the computed values underestimate the

« true » resuspension fluxes that would have been estimated dead astern of the trawl. The effect of the time delays on the resuspension fluxes will be discussed in section 3.6.

Sediment resuspension fluxes were observed to decrease with increasing sediment grain size. Maximum fluxes were estimated around 540 g m^{-2} s^{-1} for the finest sediment at SC90 site, and they range from 150 to 210 g m^{-2} s^{-1} for the coarser sediment at SC30 site (Table 3). Taking into account the probable bias due to the time delay between plume generation and initial data collection, it appears that largest resuspension fluxes were obtained for the Rockhopper trawl. The calculated equivalent thickness of sediment that must be eroded to produce the resuspended load from the seabed ranges between 0.1 and 0.4 mm (Table 3).

3.4 Particle size distribution

Due to the importance of the Rockhopper trawl in producing the largest resuspension fluxes, the following particle size data presentation is for the Rockhopper trawl experiment at CS60 site only, but the LISST-generated particle size distribution (PSD) results are valid for all sites and bottom trawls. Depth-averaged PSD completed in the laboratory for sonicated, surficial (0-10 cm) sediment samples and suspended particle samples collected on filters both inside and outside the plume showed similar bi-modal PSD (Fig. 9a). Conversely, depth-averaged *in situ* PSD both inside and outside the plume were significantly different. They showed a quasi-absence of clays, a reduced abundance of fine silts, and an increasing fraction of particles larger than 10, 20, and 60 µm (for SC90, CS60 and CS30 sediments, respectively) with a large peak between 150 and 200 µm (Fig. 9b). The discrepancy between *in situ* and laboratory distribution suggests the presence in the bottom water layer of flocs built up from clayey and silty individual particles.

PSD were identical for various depths outside the sediment plume (Fig. 10a), but showed a substantial spatial (vertical) and temporal variations inside the plume (Fig. 10b and 11). For a

single downcast, the abundance of the large (150-200 µm) particle flocs was maximal at the top of the plume and decreased closer to the seabed (Fig. 10b). The abundance of smaller, 30-100 µm flocs displayed an opposite trend: their abundance was maximum near the seabed and decreased farther from the seabed (Fig. 10b). Furthermore, PSD obtained at few minutes intervals and at a constant depth (1.5 m) above the seabed within the same plume showed rapid changes of the abundance ratio between the 30-100 µm and 150-200 µm flocs (Fig. 11). While the volume concentration of small flocs was larger than that of the large flocs at the initial collection time, the ratio was inverted less than 10 minutes later.

3.5 Fluxes of particulate and dissolved elements

The resuspension of sediment by trawls provoked a strong increase of POC, PN concentrations in the lower part of the plume (2-3 m a.b, Fig. 12c-d). The quantity of POC and PN injected into the bottom water layer appeared to be maximized by the Rockhopper trawl relative to the Medits trawl (Table 3). Resuspension fluxes ranged between 1.4 and 4.6 g m^{-2} s^{-1} for POC and between 0.2 and 0.7 g m^{-2} s^{-1} for PN and these fluxes decreased with increasing sediment grain size as represented by the three sites (Table 3).

A significant increase was observed for nitrate+nitrite (Table 4) and DOC (data not shown) concentrations within the turbid plume. For phosphate and silicate, the increase was slight but generally close to the accuracy of the analytical methods (Fig. 12 e-h, Table 4). Variations of ammonium, DON and DOP concentrations were in most cases not significant. The nutrient fluxes, averaged over all sites and trawl-types, are about 1400 µmol m^{-2} s^{-1} for nitrate+nitrite, 55 µmol m^{-2} s^{-1} for ammonium, 80 µmol m^{-2} s^{-1} for phosphate and 1050 µmol m^{-2} s^{-1} for silicate (Table 5).

The equivalent sediment thickness required to be resuspended to provide the estimated POC and PN influx represent a layer less than one millimetre thick, as for resuspended sediment

(Table 3). For dissolved elements, this layer was much thicker (between 1 to more than 10 cm, Table 4).

3.6 Redeposition of turbid plumes

The settling and dispersal of sediment plumes were traced twice. In the first case (CS30, site with the coarsest sediment), the plume segment generated by a professional bottom trawler was transected four times during a total period of 4 hours (Fig. 13a). The mean current perpendicular to the path of the trawl was low (< 4 cm s^{-1}) but instantaneous currents were stronger (up to 14 cm s^{-1}) and highly variable due to windy conditions. The plume remained centred around its original track, and underwent a significant lateral spreading from 30 m to 480 m after 4 hours. In the second case (SC90, site with the finest sediment), the four successive and parallel plumes were transected once and the oldest plume was measured at 3 hours 30 (Fig. 13b). The bottom currents, oriented across the path of the trawl, were unidirectional and constant (~ 3 cm s^{-1}). Due to the low current fluctuations, the lateral spreading of the plumes was small and they essentially retained the width of the initial plume (~ 200 m) while they were advected by the mean current. The sediment load for both plumes rapidly collapsed by about one to two-thirds respectively after 30 minutes, but between one-tenth to one-third of the initial load remained in suspension after 3-4 hours (Fig. 14a and b).

Given the rapid decay at the early stage of the plume, it appeared crucial for a correct estimation of the initial sediment load to take into account the amount of particulate matter that settled on the seabed during the time delay. Figure 14 shows the decay curves of the deposition expression fitted to the temporal mass changes measured during the plume monitoring at both sites. The regression fit led to an initial mass of resuspended sediment M_0 of 6.9 kg for the professional trawler at CS30 site and 28.3 kg for the Medits trawl at SC90 site. These values represented an increase of 5 to 27% with respect to the estimates

established for the first crossing of the plume. Using estimate of E calculated for the ambient conditions recorded for each monitoring (8×10^{-6} m^2 s^{-1} at CS30, 6×10^{-6} m^2 s^{-1} at SC90), these values of E led to estimate of W_s of 5×10^{-5} m s^{-1} and 3×10^{-5} m s^{-1} for the CS30 and SC90 sites respectively, which corresponds to typical settling velocities for fine sediment flocs (Eisma et al., 1996).

4. DISCUSSION

4.1 Characteristics of trawl-induced turbid plumes

The characteristics of the sediment plumes generated by the bottom trawls agree with earlier observations. The height of the plume, which is about twice the vertical opening of the trawl net, is similar to that observed by Main and Sangster (1981) for sandy sediment. The maximum SSC observed at 0.5 m a.b. in the sediment plumes (between 150 and 300 mg l^{-1}) are close to the observations of Schoellhammer (1996), in which an SSC value of 250 mg l^{-1} was observed between 0.27 and 0.46 m a.b., downstream of the trawling line. Such SSC are comparable to the near-bottom SSC observed at 26 m during a severe storm in the Gulf of Lion (Ferré et al, this volume).

The asymptotic decrease of suspended sediment load within the plume agrees with observations of Schoellhammer (1996) and Palanques *et al*. (2001), who reported that some of the resuspended sediment remained in suspension for at least 8 hours and even during 2 days. The regression fit of the plume load decay at the CS30 and SC90 sites leads to a revaluation of resuspended mass of sediment.

The initial mass for each trawling experiment was estimated using the local vertical dispersion coefficient (calculated from measured density and velocity profiles) and an average settling velocity (4×10^{-5} m s^{-1}). It appears that the excess masses, resuspension fluxes and equivalent

sediment thicknesses summarized in Table 3 are underestimated by 2 to 30%. Resuspension fluxes by bottom trawls are thus estimated to range between 190 mg m^2 s^{-1} and 800 mg m^2 s^{-1} and with an average of 410 mg m^2 s^{-1}. Likewise the average resuspension of POC and PN are estimated to 3.6 mg m^2 s^{-1} and 0.6 mg m^2 s^{-1} respectively.

The equivalent sediment thickness required to be resuspended to provide the estimated sediment, PN and POC influx represent thus a layer less than one millimetre thick. For nutrients, this layer was at least a few centimetres thick (between 0.4 and 10 cm). While these latter values were more in accordance with the expected sediment thickness to be disturbed by doors and groundrope of bottom trawls, the first value indicated that only a small fraction of the sediment actually remobilised by the trawls is resuspended and dispersed in the bottom water layer.

LISST-measured PSD inside and outside the plumes clearly indicate the presence of fine particle (clay and silt) flocs populations of 30-100 µm and 150-200 µm, which are commonly found in the estuarine and coastal waters (Eisma et al., 1996 and the references therein). The vertical distribution and the short term temporal change of flocs size, with a higher abundance of small flocs at the bottom and at the early stage of the plume, are most probably the result of higher turbulence shear of the fluid close to the seabed in the wake of the trawl. Indeed, Manning and Dyer (1999) showed that, while increasing SSC at low shear level favoured floc growth, increasing SSC together with increasing turbulent shear disrupted of the flocculation process. The reproducibility and vertical homogeneity of PSD measured outside the plumes (Fig. 10a) over the period of the experiment, suggests that the floc size distribution of resuspended sediment eventually evolved toward a more or less vertically homogeneous and average abundance.

4.2 Impact of dissolved nutrient injection

Our results showed that trawling inject significant quantities of nutrients (nitrate + nitrite especially) in the water column. The trawling-induced nutrients fluxes are 2 to 5 orders of magnitude larger than the average natural fluxes measured over the Gulf of Lion shelf (Denis and Grenz, 2003) or the North Sea (Tengberg *et al.*, 2003) (Table 5). Natural nutrients effluxes from the Gulf of Lion sediments are known to be weak, mainly due to the low organic contents of the sediments, and to show low temporal and spatial variability (Denis and Grenz, 2003). Tengberg *et al.* (2003) also estimated the impact of artificial resuspension (stirring with paddle wheel in benthic chambers) on the nutrient fluxes. They observed that the fluxes of nitrate+nitrite and silicate strongly increased after resuspension (Table 5). Nevertheless, these resuspension fluxes are still several orders of magnitude lower than the trawling-induced fluxes. This difference likely relates to the thickness of sediment resuspended, which was about few µm for the chamber resuspension (Tengberg *et al.*, 2003) and few centimetres for the trawling resuspension.

This latter study and our results both show that, wheareas nitrate+nitrite and ammonium are more concentrated in the sediment than in the bottom water layer, only nitrate+nitrite concentrations significantly increase in the water layer after resuspension. The constancy of ammonium concentrations might be related to the absorption of the resuspended ammonium on particles, due to the propping effects of hydroxycation islands in the interlayer spaces of clays. Ammonium exchange is a rapid and reversible process (Boatman and Murray, 1982) and exponential when concentration increases (Suess and Muller, 1981). Moreover, nitrifers are closely associated with particle surfaces when available (Keen and Prosser, 1988). The release of ammonium by resuspension can be hampered by the enrichment in SPM and associated NH_4^+ oxidizing bacteria.

Sediment resuspension can thus enrich the water column with nutrients, which are immediately available for autotrophic or heterotrophic activity (Fanning et al. 1982; Simon, 1989). The impact of these nutrients on the ecosystem will strongly depend upon the environmental conditions. Indeed, if the water column is already rich in nutrient such as in winter, in frontal zone, in upwelling, or in deep cold water water (Pujo-Pay and Conan, 2003), the introduction of new nutrients will not modify significantly the functioning of the biological communities. Conversely, in a water column depleted in nutrients such as in summer and in offshore water (Pujo-Pay and Conan, 2003), the injection of new nutrients could locally generate a bloom and prime a population succession because of phosphate or nitrate limitation of the production (Conan et al., 1999). Thus dissolved nutrient injection by bottom trawling activity in shallow waters and summer period might impact the biological production of the Gulf of Lion.

5. CONCLUSIONS

This study focused on the impact of trawls on the resuspension of cohesive muddy sediment and associated elements led to the following conclusions:

1. Bottom trawls causes a significant resuspension of sediment, while the near-bottom pelagic trawls towed at 10 or 1 m above the seabed have no impact on the sediment. Otter doors and the net contribute both to the resuspension. The observed release of dissolved elements (nutrients) suggest that trawl gears scrape at least the top few centimetres of the sediment. Nevertheless, only a small fraction of the remobilised sediment (corresponding to a layer less than one millimetre thick) is effectively injected as suspended particulate matter in the water column.
2. Resuspended sediment clouds at several hundreds meters stern of trawls are few metres high (average 4 m), 70-200 m wide, and exhibited average excess SSC between 10 and

50 mg l^{-1}. The combination of integrated load over a segment of the plume with the trawl horizontal opening and trawler speed yield the resuspension fluxes. The estimated suspension fluxes for sediment, including corrections for missing near-bottom data and time delay between plume generation and initial data collection , lie in the range 190-800 g m^{-2} s^{-1} (average 410 g m^{-2} s^{-1}). The higher values are associated with the finest sediments and the Rockhopper trawl. Fluxes of particulate elements and nutrients depend on the concentration gradient of these elements between the sediment and the near-bottom water. In this study, approximate fluxes of nutrients induced by trawls were 2 to 5 orders of magnitude higher than the natural diffusive effluxes.

3. The decay and spreading of turbid plumes is dependent of the settling velocity spectra of the suspended materials, the vertical dispersion, and the variability of the horizontal currents in the bottom boundary layer. The dynamics of aggregated material appears to be a key point for settling of the sediment plume. A large fraction (one to two-thirds) of the sediment load settles during the first hour after the passage of the trawl, but about one-tenth remains in suspension. The sediment puffs generated by bottom trawls are thus likely to regularly feed the bottom nepheloid layer with suspended fine-grained sediment, particulate and dissolved elements.

These results will be included in an on-going study on the modelling of the impact of a trawler fleet on the resuspension and dispersal of sediment and particulate organic matter on the Gulf of Lion continental margin.

ACKNOWLEDGEMENTS

This work was supported by funding under the European INTERPOL project (# EVK3-2000-00526). The authors would like to thank the technicians of the CEFREM (P. Barthe, J.L. Blazi, J. Carbonne, G. Saragoni) and of the LOBB (L. Oriol, M. Girodengo, C. Durmez) for

their assistance during the preparation and the realisation of the fieldwork. We also deeply thank the captains and crews of the R/V Tethys II and l'Europe whose enthusiasm and ability to manoeuvre largely contributed to the success of this study. C.H. Pilskahn and an anonymous reviewer are deeply thanked for their comments and suggestions that greatly improve the manuscript.

REFERENCES

Agrawal, Y.C., Pottsmith, H.C., 2000. Instruments for particle size and settling velocity observations in sediment transport. Marine Geology, 168, 89-114.

Blackburn, T.H., 1991. Mineralization in northwestern Mediterranean Sea sediments : Cybele cruise. In EROS 2000 (European River Ocean System) Project workshop Den Burg/Texel 21-25 october 1991, eds J.M. Martin and H. Barth. Water Pollution Research Report 28, CEC Directorate –General for Science, Research and development, Brussels, pp. 469-479.

Blackburn, T.H., 1993. Nitrogen cycling in NW Mediterranean sediments. In EROS 2000 (European River Ocean System) Project workshop Plymouth 28 september – 2 october 1992, eds J.M. Martin and H. Barth. Water Pollution Research Report 30, CEC Directorate – General for Science, Research and development, Brussels, pp. 225-229.

Boatman, C.D. and Murray, J.W., 1982. Modeling exchangeable NH_4^+ adsorption in marine sediments: Process and controls of adsorption. Limnology and Oceanography, 27 (1), 99-110.

Buscail, R., Pocklington, R., Germain, C., 1995. Seasonal variability of the organic matter in a sedimentary coastal environment : sources, degradation and accumulation (continental shelf of the Gulf of Lions – Northwestern Mediterranean Sea). Continental Shelf Research, 15 (7), 843-869.

Cauwet G. (1994). HTCO method for dissolved organic carbon analysis in seawater: influence of catalyst on blank estimation. *Marine Chemistry*, **47** (1): 55-64

Churchill, J.H., 1989. The effect of commercial trawling on sediment resuspension and transport over the middle Atlantic Bight continental shelf. Continental Shelf Research, 9 (9), 841-864.

Churchill, J.H., 1998. Sediment resuspension by bottom fishing gear. In: Dorsey E. M. and Pederson J. (Eds.), Effects of Fishing Gear on the Sea Floor of New England. Conservation Law Foundation, pp 134-137.

Conan, P., Turley, C. M., Stutt, E., Pujo-Pay, M., Van Wambeke, F., 1999. Relationship between Phytoplankton Efficiency and the Proportion of Bacterial Production to Primary Production in the Mediterranean Sea. Aquatic Microbial Ecology, 17(2), 131-144.

Denis, L., Grenz, C., 2003. Spatial variability in oxygen and nutrient fluxes at the sediment-water interface on the continental shelf in the Gulf of Lions (NW Mediterranean). Oceanologica Acta, 26 (4), 373-389.

Diaz, F., Conan, P., Raimbault, P., 2000. Small-scale study of primary productivity during spring in a Mediterranean coastal area (Gulf of Lions). Continental Shelf Research, 20, 975-996.

Durrieu de Madron, X., Abassi, A., Heussner, S., Monaco, A., Aloisi, J.C., Radakovitch, O., Giresse, P., Buscail, R., Kerhervé, P., 2000. Particulate matte rand organic carbon budgets for the Gulf of Lions (NW Mediterranean). Oceanologica Acta, 23 (6), 717-730.

Durrieu de Madron, X., Panouse, M., 1996. Transport de matière en suspension sur le plateau continental du Golfe du Lion - Situation estivale et hivernale. Comptes Rendus de l'Académie des Sciences, Série IIa, Paris, 322, 1061-1070.

Eisma, D., Bale, A.J., Dearnaley, M.P., Fennessy, M.J., Van Leussen, W., Maldiney M.-A., Pfeiffer A., Wells, J.T., 1996. Intercomparison of in situ suspended matter (floc) size measurements. Journal of Sea Research, 36, 3-14.

Fanning K.A., Carder K.L., Betzer P.R., 1982. Sediment resuspension by coastal waters: a potential mechanism for nutrient re-cycling on the ocean's margins. Deep Sea Research, 29, 953-965

Ferré, B., Guizien, K., Durrieu de Madron, X., Palanques, A., Guillén, J., Grémare, A. Fine-grained sediment dynamics during a strong storm event in the inner shelf of the Gulf of Lion (NW Mediterranean). Continental Shelf Research. This volume

Fiorentini, L, Dremiere, P.Y., Leonori, I., Sala, A., Palumbo, V., 1999. Efficiency of the bottom trawl used for the Mediterranean international trawl survey (MEDITS). Aquatic Living Resources, 12 (3), 187-205.

Fiorentini, L., Cosimi, G., Sala, A., Palumbo, V. and Leonori, I., 1996. Intercalibration des campagnes internationales de chalutage démersales en Méditerranée centrale. IRPEM. CE Med/93/015, pp. 59.

Floderus, S, Pihl, L, 1990. Resuspension in the Kattegat: Impact of variation in wind climate and fishery. Estuarine, Coastal and Shelf Science, 31, 487-498.

Helder, W., 1989. Early diagenesis and sediment-water exchange in the Golfe du Lion. In EROS 2000 (European River Ocean System) Project workshop Paris 7-9 March 1989, eds J.M. Martin and H. Barth. Water Pollution Research Report 13, CEC Directorate –General for Science, Research and development, Brussels, pp. 87-101

Jones, J.B., 1992, Environmental impact of trawling on the seabed: A review. New Zealand Journal of Marine and Freshwater Research, 26 (1), 59-67.

Keen, G.A., Prosser, J.I., 1988. The surface growth and activity of Nitrobacter. Microbial Ecology, 15, 21-39.

Koroleff, F., 1969. Direct determination of ammonia in natural waters as indophenol blue. International Council for the Exploration of the Sea C. M. C., 9.

Land, J.M., Bray, R.N., 2000. Acoustic measurement of suspended solids for monitoring of dredging and dredged material disposal. Journal of Dredging Engineering, 2 (3), 1-17.

Main, J., Sangster, G.L., 1981. A study of sand clouds produced by trawl boards and their possible effect on fish capture. Scottish fisheries Research Report no 20, Dept of Agriculture and Fisheries for Scotland, pp. 19.

Manning, A.J., Dyer K.R., 1999. A laboratory examination of floc characteristics with regards to turbulent shearing. Marine Geology, 160, 147-170.

Morgan, L.E., Chuenpagdee, R., 2003. Shifting gears: addressing the collateral impacts of fishing methods in U.S. waters. Pew science series on conservation and the environment. Island Press Publication Services. pp. 42.

Mullin, J.B., Riley, J.P. 1955. The spectrophotometric determination of silicate-silicon in natural water with special reference to seawater. Analytica Chimica Acta, 12, 162-170

Murphy, J., Riley, J. P., 1962. A modified single solution method for determination of phosphate in natural water. Analytica Chimica Acta, 27, 37-36.

Nedelec , C. and J. Prado, 1990. Definitions and classification of fishing gear categories. FAO Fisheries Technical Paper, 222 (Rev. 1), pp 92.

Palanques, A., Guillén, J., Puig, P., 2001. Impact of bottom trawling on water turbidity and muddy sediment of an unfished continental shelf. Limnology and Oceanography, 46 (5), 1100-1110.

Peng, T-H, Broecker, W.S., 1984. Ocean life cycles and the atmospheric CO_2 content. Journal of Geophysical Research, 89 (C5), 8170-8180.

Pilskaln, C.H., Churchill, J.H., Mayer, L.M,. 1998. Resuspension of Sediment by Bottom Trawling in the Gulf of Maine and Potential Geochemical Consequences. Conservation Biology. Vol. 12 (6), 1223-1229.

Prandle, D., 1997. Tidal characteristics of suspended sediment concentrations. *Journal of Hydraulic Engineering*, 123 (4), 341-350

Pujo-Pay M., Raimbault P., 1994. Improvement of the wet-oxydation procedure for simultaneous determination of particulate organic nitrogen and phosphorus collected on filters. Marine Ecology Progress Series, 105, 203-207

Pujo-Pay, M., Conan, P., 2003. Seasonal variability and export of dissolved organic nitrogen in the northwestern Mediterranean Sea. Journal of Geophysical Research, 108, C6, 1901-1911.

Rester J.K., 2000. Annotated bibliography of fishing impacts on habitat. Gulf States Marine Fisheries Commission. Number 73. Ocean Springs, Mississipi, 168 p.

Riemann, B., Hoffman E, 1991. Ecological consequences of dredging and bottom trawling in the Limfjord, Denmark. Marine Ecology Progress Series, 69, 171-178.

Schoellhamer, D.H., 1996. Anthropogenic sediment resuspension mechanisms in a shallow microtidal estuary. Estuarine, Coastal and Shelf Science, 43 (5), 533-548

Simon N.S., 1989. Nitrogen cycling between sediment and the shallow water column in the transition zone of the Potomac river and estuary. II. The role of wind driven resuspension and absorbed ammonium. Estuarine, Coastal and Shelf Science, 28, 531-547

Suess, E., Muller, P.J., 1981. Interaction between K+ and NH4+ in marine pore solution and sediments. Geochimica and Cosmochimica Acta, 45, 1581-1602.

Tengberg, A., Almroth, E., Hall, P., 2003. Resuspension and its effect on organic carbon recycling and nutrient exchange in coastal sediments: *in situ* measurements using new experimental technology. Journal of Experimental Marine Biology and Ecology, 285-286, 119-142.

Tréguer, P., Le Corre, P., 1975. Manuel d'analyses des sels nutritifs dans l'eau de mer. Laboratoire d'Océanographie Chimique. Université de Bretagne Occidentale, Brest, pp. 110.

Watling, L. and Norse, E.A., 1998. Disturbance of the seabed by mobile fishing gear: a comparison to forest clearcutting. *Conservation Biology*, 1180-1197.

Wood, E.P.K., Armstrong, F.A.J., Richards F.A., 1967. Determination of nitrate in seawater by cadmium cooper reduction to nitrite. Journal of Marine Biological Association of United Kingdom, 47, 23-31.

Figure Captions

Figure 1 Diagram of fishing vessel (a) towing a bottom trawl and (b) a pelagic trawl over the seabed.

Figure 2. Map of the study area in the Gulf of Lion continental shelf. The three study sites are indicated as CS30 (clayey silt site at 30 m depth), CS60 (clayey silt at 60 m depth) and SC90 (silty clay site at 90 m depth)

Figure 3. Top and side views of the arrangement and moving of ships to characterise to sediment plumes generated by a bottom trawl.

Figure 4. Example of simultaneous SSC profiles measured from water samples, light-transmission measurements and acoustic backscattering measurements in a Rockhopper turbid plume on the SC90 site.

Figure 5. Sketch of the sampled box, of length L, height H and width l, across a segment of a turbid plume generated by a bottom trawl. The x-axis is along the transect, the y-axis is along the trawl path, the z-axis is oriented vertically. The dashed line delineates the suspended sediment plume, and the shaded strips at the bottom define the areas scraped by the groundrope and the otter doors of the trawl.

Figure 6. Suspended sediment concentration (in mg l^{-1}) distribution along transects of sediment plumes generated by (a) a Medits bottom trawl in abnormal working conditions (weak contact with seabed) at CS30 site, and (b) a Rockhopper trawl in normal working conditions at SC90 site. The bottom scales indicate the elapsed time since the passage of the trawl and the distance covered by the ship towing the ADCP.

Figure 7. Profiles of SSC (in mg l^{1}) before trawling and maximum SSC within the plume generated by three types of bottom trawlers (Medits otter trawl, Rockhopper trawl, and professional trawl) on (a) clayey silt sediment at 30 m depth (CS30 site), (b) clayey silt sediment at 60 m depth (CS60 site) and (c) silty clay sediment at 90 m depth (SC90 site).

Figure 8. Comparative average particle size-distribution from LISST for surface sediments, and filtered suspended particle samples collected between 1.4 and 5.4 m a.b. outside and inside a plume at CS60 site using a rockhopper trawl: (a) laboratory PSD for sonicated samples, (b) *in situ* measurements of PSD.

Figure 9. Vertical distribution of *in situ* particle size-distribution measured during two downcasts (a) outside and (b) inside a sediment plume generated by a Rockhopper trawl at CS60 site.

Figure 10. Variation of in-situ particle size-distribution measured at 1.5 m a.b. at different time after the initial data collection within a sediment plume generated by a Rockhopper trawl at CS60 site.

Figure 11. Example of hydrological profiles (T, S, fluorescence, SSC) and nutrients (NO_3+NO_2, NH_3, PO_4, $Si(OH)_4$) in the whole water column before trawling at CS60 site.

Figure 12. Example of profiles of particulate matter (SSC, TN, POC), fluorescence and nutrients (NO_3+NO_2, NH_3, PO_4, $Si(OH)_4$) in the near-bottom layer outside and inside a sediment plume generated by a Rockhopper trawl at CS60 site.

Figure 13. (a) Distribution of a plume segment at various time after its generation by a professional bottom trawl at 30 m depth (CS30 site), estimated from acoustic measurements. The plume resulted from a single haul by a professional bottom trawl that was transected at various times after its generation. (b) Distribution of a plume segments at various time after their generation by a Medits bottom trawl at 90 m depth (SC90 site), estimated from acoustic measurements. The plumes resulted from successive parallel hauls that are transected all at once.

Figure 14. Total sediment load within a plume segment at various time after the generation of the plume by (a) a professional trawl at 30 m depth (CS30 site) and (b) a Medits trawl at 90 m depth (SC90 site). The solid line indicates the simulated sediment load variation.

Table Captions

Table 1. Characteristics of the GOC73 (Medits and Rockhopper otter trawls) and of the PTGM 158 (pelagic trawl). Professional bottom trawls in the Gulf of Lion have heavier doors (up to 800 kg), a smaller wing aperture (5-8 m) and higher speed over the ground (3.8 – 4.2 knots)

Table 2. Average grain size and range of chemical element concentrations in the upper 10 cm of the sediment for the three study sites: clayey silt sediments (CS30 and CS60 sites), silty clay sediment (SC90 site), and parameters used to calibrate ADCP signal for the different sites.

Table 3. Characteristics of the trawl geometry and sediment plume geometry, and estimates of the resuspension fluxes of particulate matter and equivalent sediment thickness for the three study sites and the different bottom trawls. The equivalent sediment thickness represents the layer of sediment containing as much suspended sediment or particulate element as the total load found within the plume segment.

Table 4. Estimates of the average excess concentration in the plume, resuspension fluxes of dissolved nutrients and equivalent sediment thickness for two study sites and different bottom trawls. Italic values are not significantly different from 0. The equivalent sediment thickness represents the layer of sediment containing as much pore water nutrients as the total load found within the plume segment.

Table 5. Comparison of natural effluxes and resuspension fluxes of nutrients from sediments in the Gulf of Lion and the North Sea.

Table 1

Device	Main characteristics
Trawl	
Type GOC73	Sampling bottom trawl, made of four panels
Floatline length	35.70 m
Groundrope length	40.00 m
Sideropes length	7.40 m
Wings meshsize	140 mm (stretched)
Codend meshsize	20 mm (stretched)
Rigging	
Doors	Morgère WH type ; 2.5 m ; 350 kg each
Sweeps	Combination rope; diameter: 32 mm; Length: 100 m (10-200m depth)
Upper bridles	Steel wire ; diameter :10 mm ; length : 30 m
Lower bridles	Combination rope ; diameter : 32 mm ; length : 29 m + 1 m chain
Floats	40 x 2.7 kgf
Groundrope gear	
(Medits)	Sinker chains : 3 x 40 kg + 15 kg
(Rockhopper)	Rubber bobbins: alternation of small and large diameter
Wing aperture	12 - 20 m
Speed over the ground	3 knots (1.5 m s^{-1})

Device	Main characteristics
Trawl	
Type PTGM	Pelagic trawl
Floatline length	65.2 m
Groundrope length	83.20 m
Wings meshsize	6000 mm (stretched)
Codend meshsize	20 mm (stretched)
Rigging	
Doors	Morgère W 2m² ; 500 kg each
Floats	16 x 3 kgf
Weight	2 x 200 kg
Sinker chains	25 kg
Speed over the ground	4.5 knots (2.3 m s^{-1})

Table 2

		SC90	CS60	CS30
	Depth (m)	90	60	30
	Porosity	0.81	0.79	0.55
Particle size	% Clay (<4 µm)	49	32	22
	% Silt	47	60	60
	% Sand (> 63 µm)	4	8	18
	D_{50} (µm)	20	30	30
Hydrology	Temperature (°C)	14	14	18
	Salinity	38	38	38
Calibration coefficients	Ks	47	46	50
	S	16	18	23
Particulate matter	POC (mg g^{-1})	10 - 7.5	12 - 10	-
	PN (mg g^{-1})	0.6 - 0.5	1.0 - 0.8	-
Dissolved matter	NO_{3+2} (µmol l^{-1})	1 - 7	4 - 130	-
	NH_4 (µmol l^{-1})	7 - 89	14 - 80	-
	PO_4 (µmol l^{-1})	1.5 - 3.2	4.5 - 8.7	-
	$Si(OH)_4$ (µmol l^{-1})	50 -160	50 - 160	-

Table 3

		SC90		CS60		CS30	
	Trawl	Medits	Rock	Medits	Rock	Medits	Rock
Trawl geometry	Towing velocity (m s^{-1})	1.5	1.5	1.5	1.5	1.5	1.5
	Wings aperture (m)	19.4	13.3	13	12.7	13	12.6
	Trawled area per second (m^2)	32.1	23.0	22.5	22.0	22.5	21.9
	Vertical opening (m)	2.4	1.9	1.9	2.3	2.1	1.9
Plume geometry	Time delay (min)	3	15	13	24	30	14
	Height (m)	> 4.2	5.5	4	4.7	3.8	2.6
	Width (m)	155	110	190	190	95	73
Suspended sediment	Integrated load (g)	17.3 10^3	12.0 10^3	4.6 10^3	7.0 10^3	3.4 10^3	4.5 10^3
	Resuspended flux (g m^{-2} s^{-1})	540	540	200	320	150	210
	Equivalent sediment thickness (mm)	0.41	0.40	0.16	0.25	0.10	0.14
Particulate organic carbon	Integrated load (g)	114.6	105.3	73.5	96.1	32.3	44.1
	Resuspended flux (g m^{-2} s^{-1})	3.6	4.6	3.3	4.4	1.4	2.0
	Equivalent sediment thickness (mm)	0.2	0.3	0.2	0.2	-	-
Particulate nitrogen	Integrated load (g)	18.6	16.6	11.1	14.9	5.1	7.0
	Resuspended flux (g m^{-2} s^{-1})	0.6	0.7	0.5	0.7	0.2	0.3
	Equivalent sediment thickness (mm)	0.6	0.8	0.3	0.5	-	-

Table 4

		SC90		CS60	
	Trawl	Medits	Rock	Medits	Rock
Nitrate + Nitrite	Average excess concentration (µmol l^{-1})	0.39	0.33	0.28	0.14
	Resuspended flux (µmol m^{-2} s^{-1})	1900	1600	1400	700
	Equivalent sediment thickness (mm)	> 100	80	> 100	10
Ammonium	Average excess concentration (µmol l^{-1})	*-0.01*	*-0.02*	0.07	*0.01*
	Resuspended flux (µmol m^{-2} s^{-1})	*-30*	*-90*	300	*40*
	Equivalent sediment thickness (mm)	-	-	15	-
Phosphate	Average excess concentration (µmol l^{-1})	0.02	0.02	0.02	*0.01*
	Resuspended flux (µmol m^{-2} s^{-1})	90	100	80	*50*
	Equivalent sediment thickness (mm)	50	55	40	-
Silicate	Average excess concentration (µmol l^{-1})	*0.06*	0.42	*0.04*	0.35
	Resuspended flux (µmol m^{-2} s^{-1})	*300*	2000	*200*	1700
	Equivalent sediment thickness (mm)	-	35	-	25

Table 5

Flux µmol m^{-2} s^{-1}	Natural flux (Denis & Grenz 2003)	Natural flux (Tengberg et al. 2003)	Paddle wheel resuspension flux (Tengberg et al. 2003)	Trawling resuspension flux (this study)
Location	Gulf of Lion	North Sea	North Sea	Gulf of Lion
Nitrate + Nitrite	$5 – 6 \times 10^{-3}$	-3×10^{-3}	6×10^{-3}	1400
Ammonium	$0.3 – 1.0 \times 10^{-3}$	2×10^{-3}	3×10^{-3}	55
Phosphate	$0.1 – 0.4 \times 10^{-3}$	0.9×10^{-3}	0.02×10^{-3}	80
Silicate	$4 – 20 \times 10^{-3}$	-13×10^{-3}	20×10^{-3}	1050

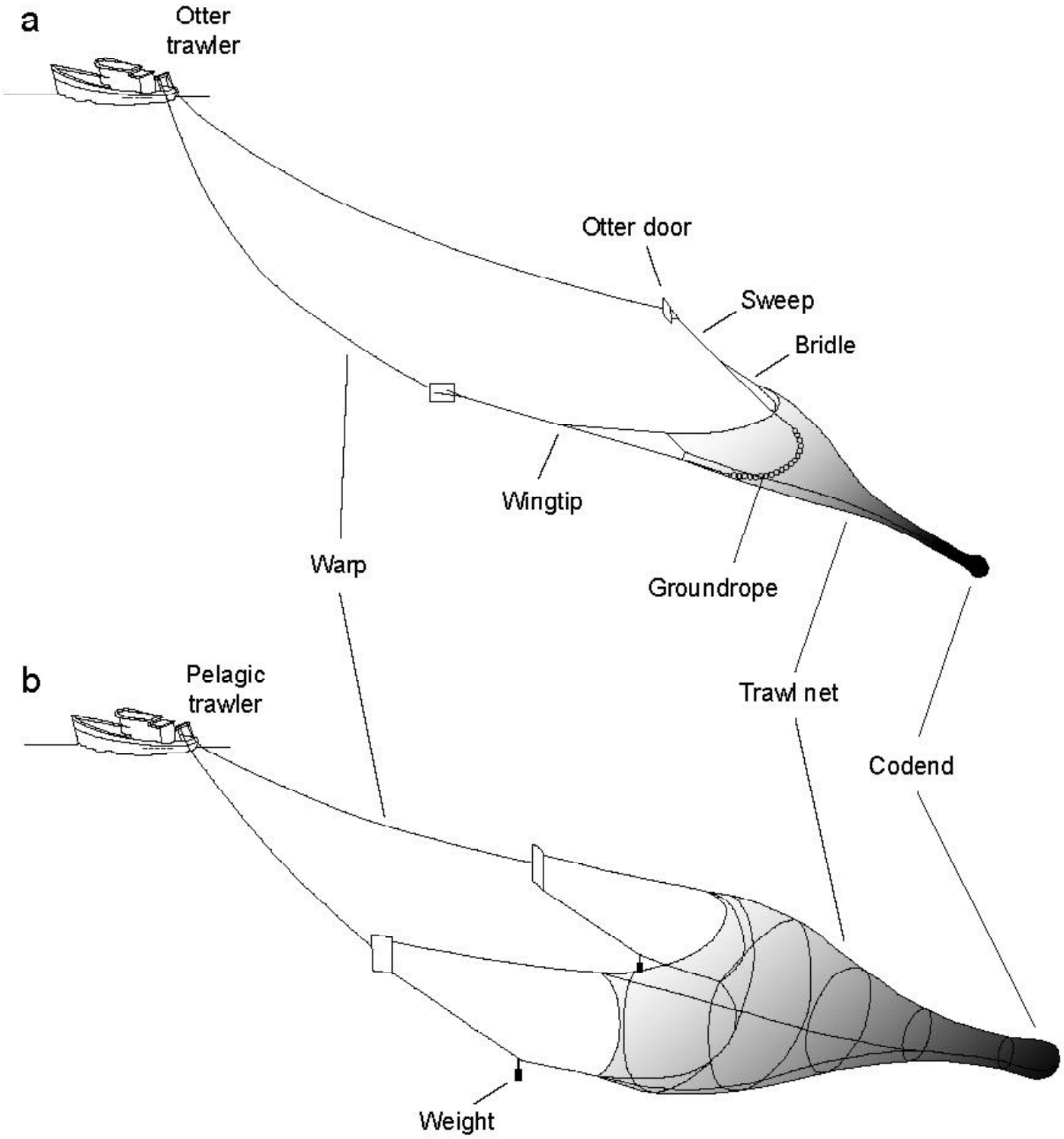
a
Otter trawler
Otter door
Sweep
Bridle
Wingtip
Warp
Groundrope
Trawl net
Codend
b
Pelagic trawler
Weight

Figure 1

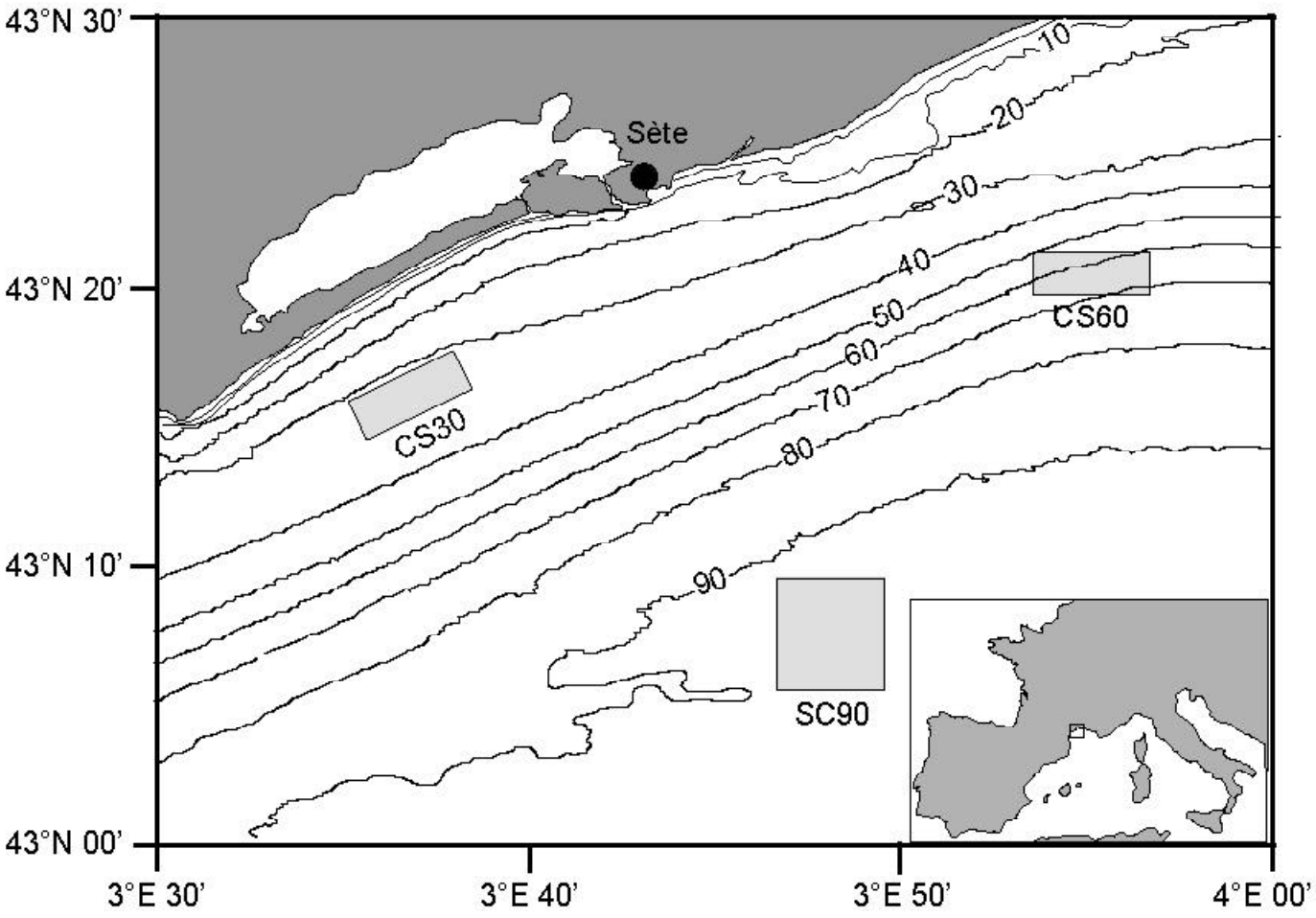
43°N 30'
43°N 20'
43°N 10'
43°N 00'
3°E 30'
3°E 40'
3°E 50'
4°E 00'
Sète
10
20
30
40
50
60
70
80
90
CS30
CS60
SC90

Figure 2

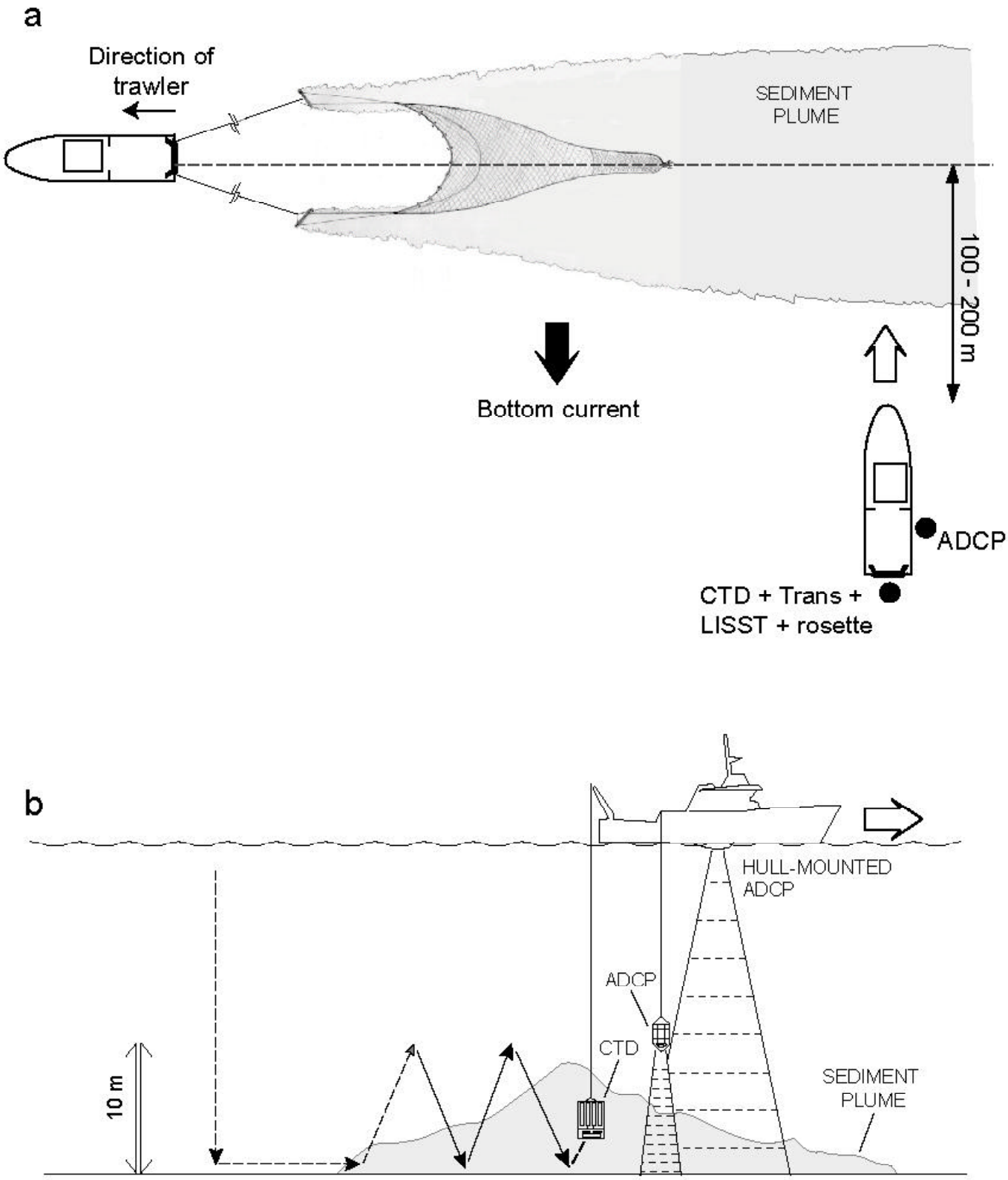
a
Direction of trawler
SEDIMENT PLUME
100 - 200 m
Bottom current
ADCP
CTD + Trans + LISST + rosette
b
HULL-MOUNTED ADCP
ADCP
CTD
SEDIMENT PLUME
10 m

Figure 3

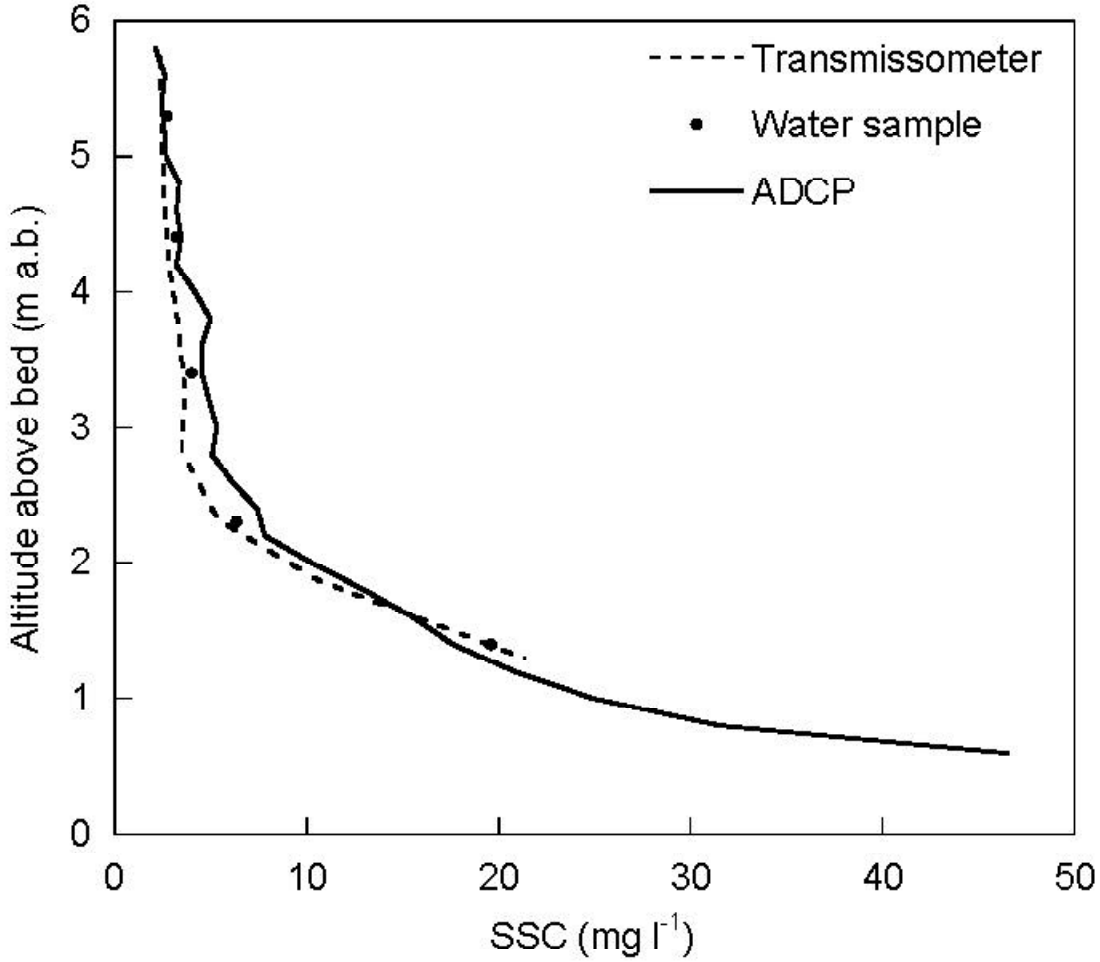
Transmissometer
Water sample
ADCP
Altitude above bed (m a.b.)
SSC (mg l-1)
0
1
2
3
4
5
6
0
10
20
30
40
50

Figure 4

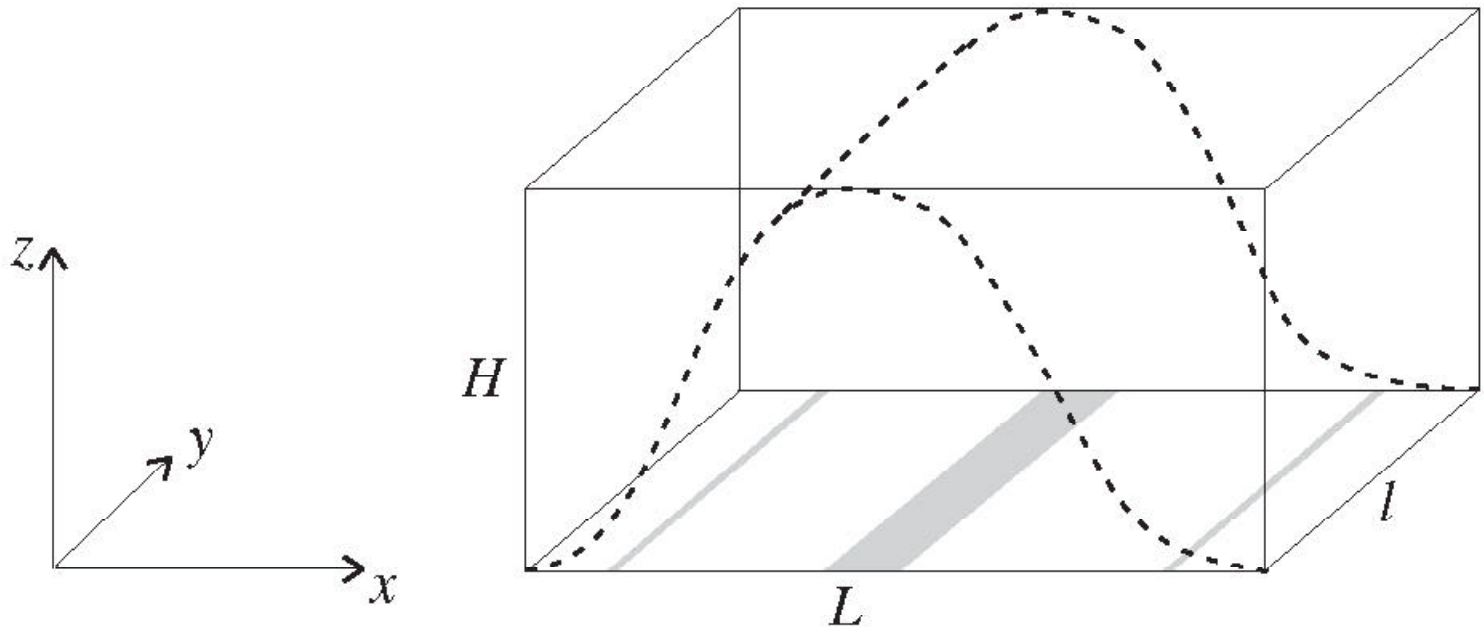

Figure 5

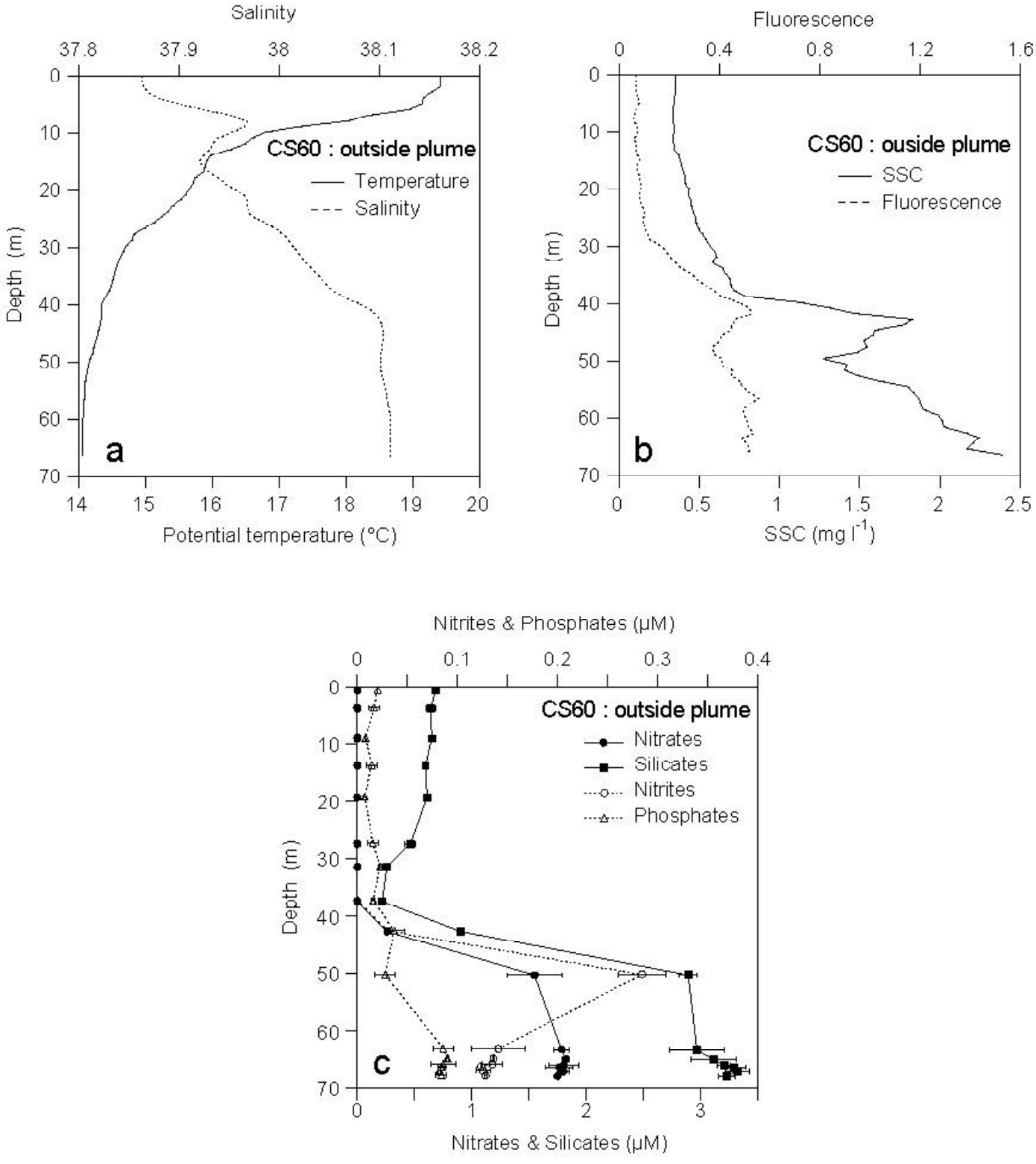
Salinity
37.8
37.9
38
38.1
38.2
Depth (m)
CS60 : outside plume
Temperature
Salinity
a
Potential temperature (°C)
Fluorescence
CS60 : ouside plume
SSC
Fluorescence
b
SSC (mg l-1)
Nitrites & Phosphates (µM)
CS60 : outside plume
Nitrates
Silicates
Nitrites
Phosphates
c
Nitrates & Silicates (µM)

Figure 6

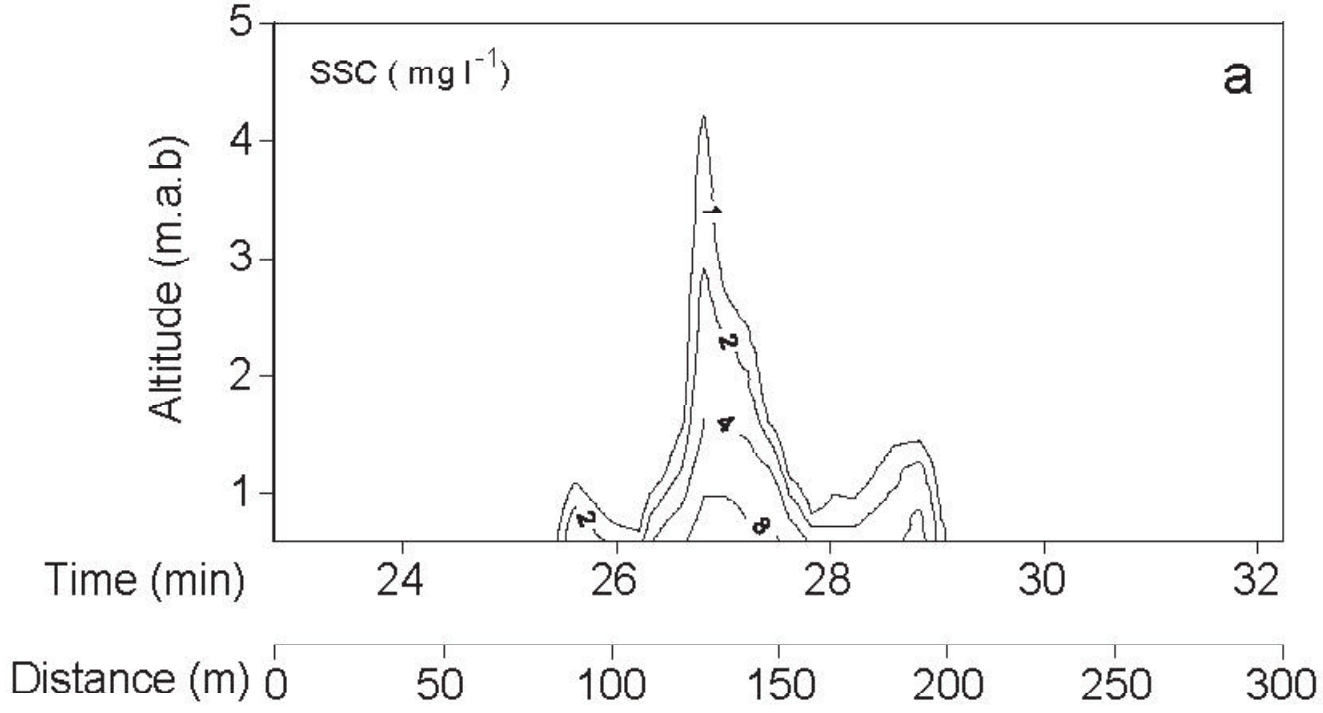
SSC (mg l^{-1})
a
Altitude (m.a.b)
5
4
3
2
1
1
2
4
8
2
Time (min)
24
26
28
30
32
Distance (m)
0
50
100
150
200
250
300

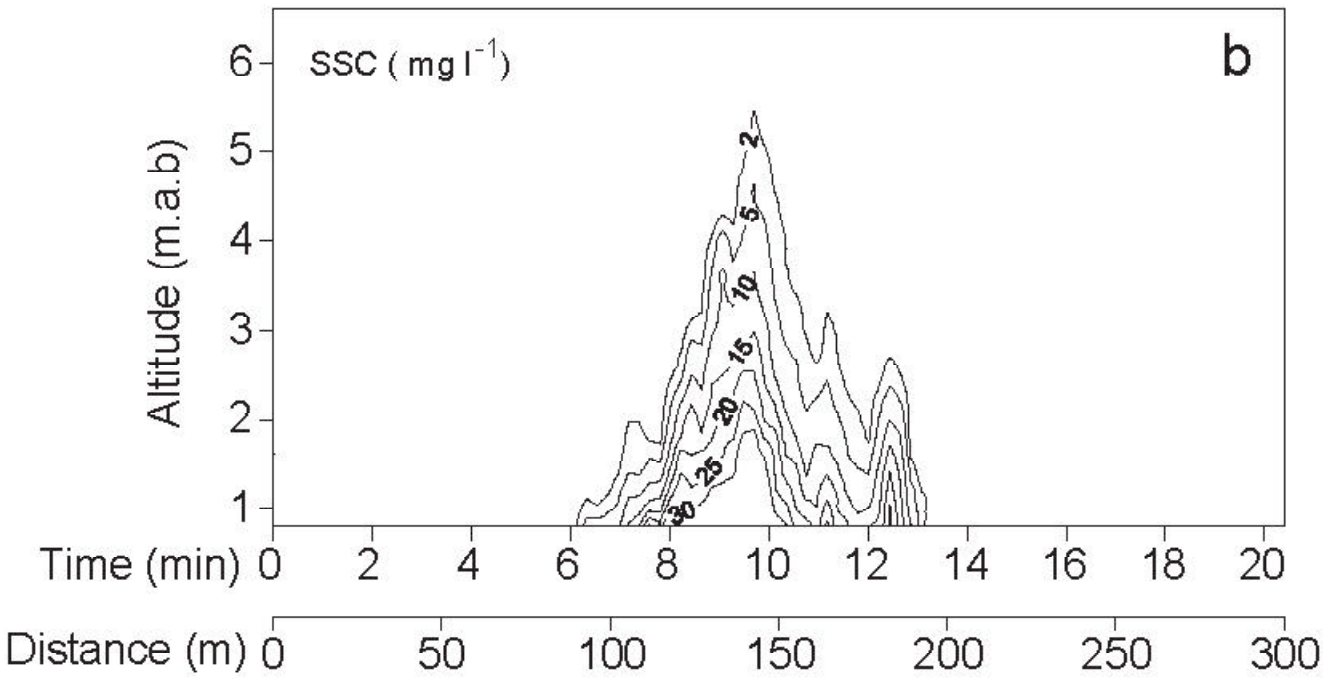
SSC (mg l^{-1})
b
Altitude (m.a.b)
6
5
4
3
2
1
2
5
10
15
20
25
30
Time (min)
0
2
4
6
8
10
12
14
16
18
20
Distance (m)
0
50
100
150
200
250
300

Figure 7

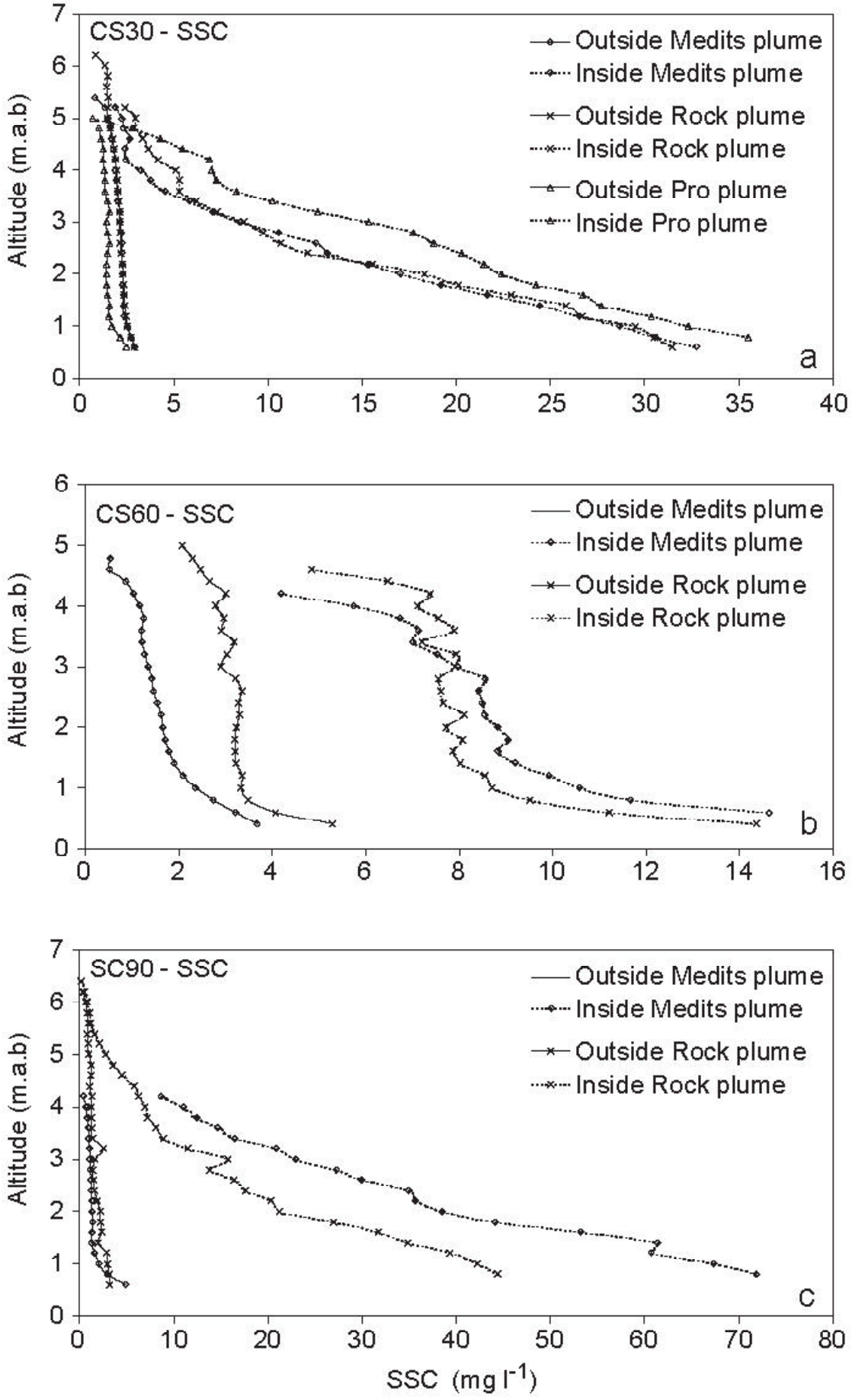
CS30 - SSC
Outside Medits plume
Inside Medits plume
Outside Rock plume
Inside Rock plume
Outside Pro plume
Inside Pro plume
Altitude (m.a.b)
a
CS60 - SSC
Outside Medits plume
Inside Medits plume
Outside Rock plume
Inside Rock plume
Altitude (m.a.b)
b
SC90 - SSC
Outside Medits plume
Inside Medits plume
Outside Rock plume
Inside Rock plume
Altitude (m.a.b)
c
SSC (mg l-1)

Figure 8

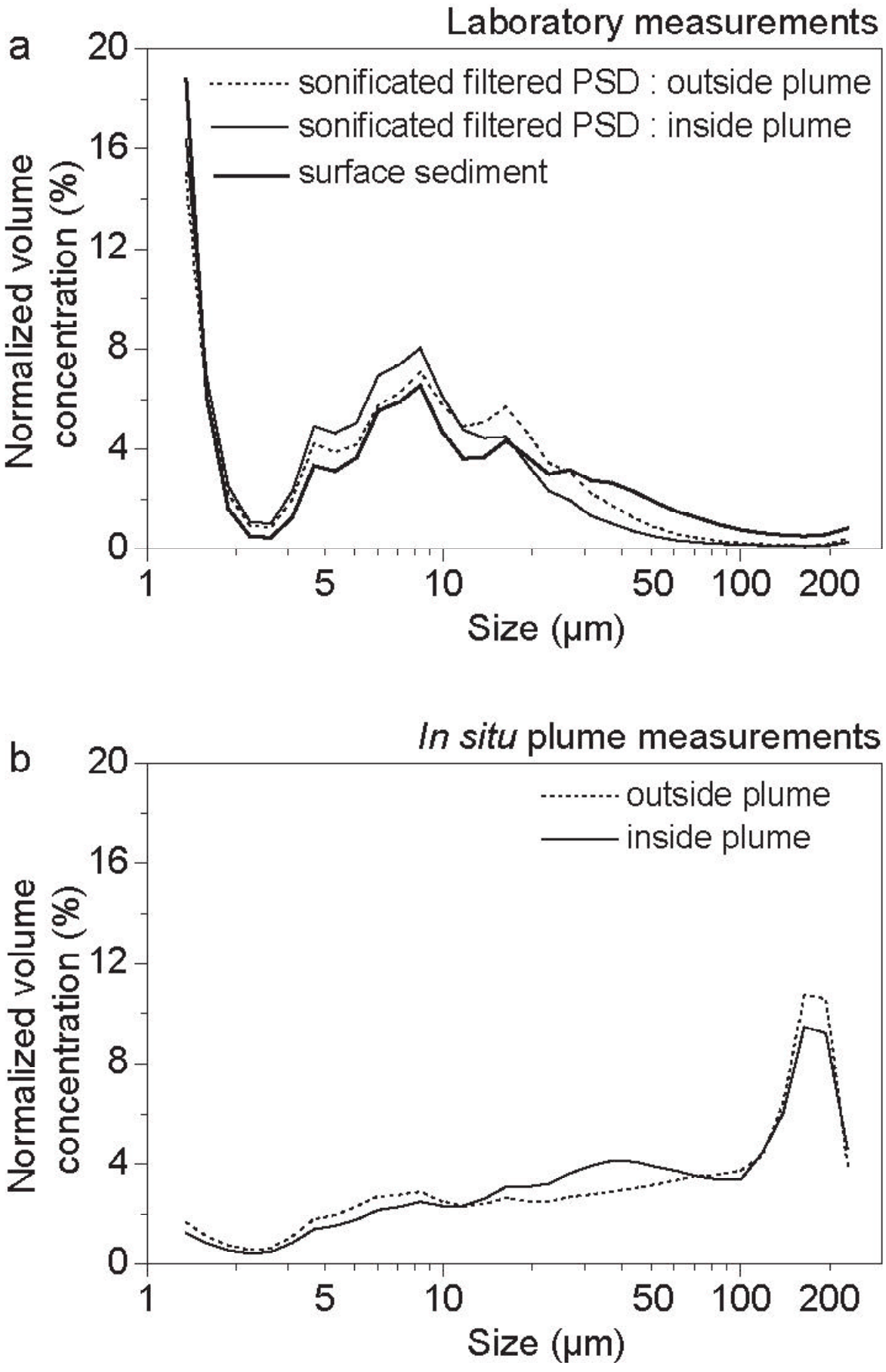
a
Laboratory measurements
sonificated filtered PSD : outside plume
sonificated filtered PSD : inside plume
surface sediment
Normalized volume concentration (%)
0
4
8
12
16
20
1
5
10
50
100
200
Size (µm)
b
In situ plume measurements
outside plume
inside plume
Normalized volume concentration (%)
0
4
8
12
16
20
1
5
10
50
100
200
Size (µm)

Figure 9

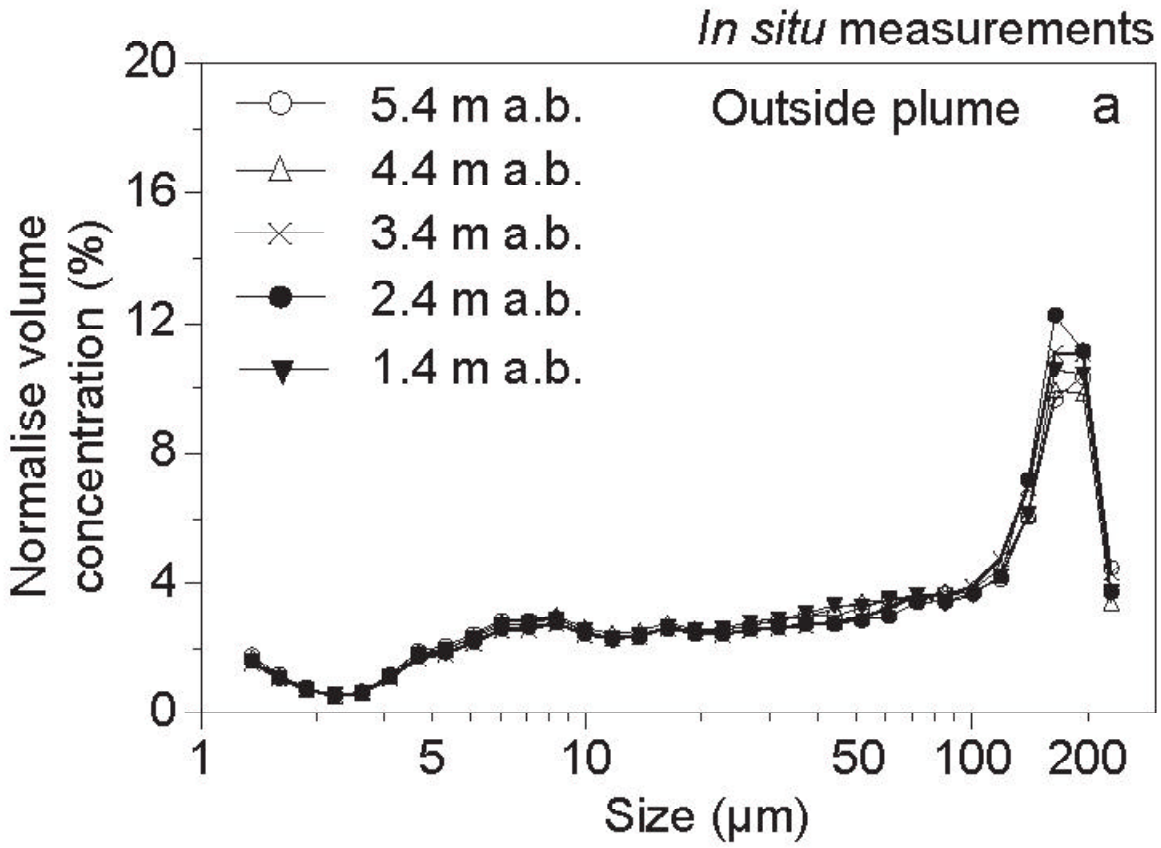
In situ measurements
Outside plume
a
5.4 m a.b.
4.4 m a.b.
3.4 m a.b.
2.4 m a.b.
1.4 m a.b.
Normalise volume concentration (%)
Size (µm)
0
4
8
12
16
20
1
5
10
50
100
200

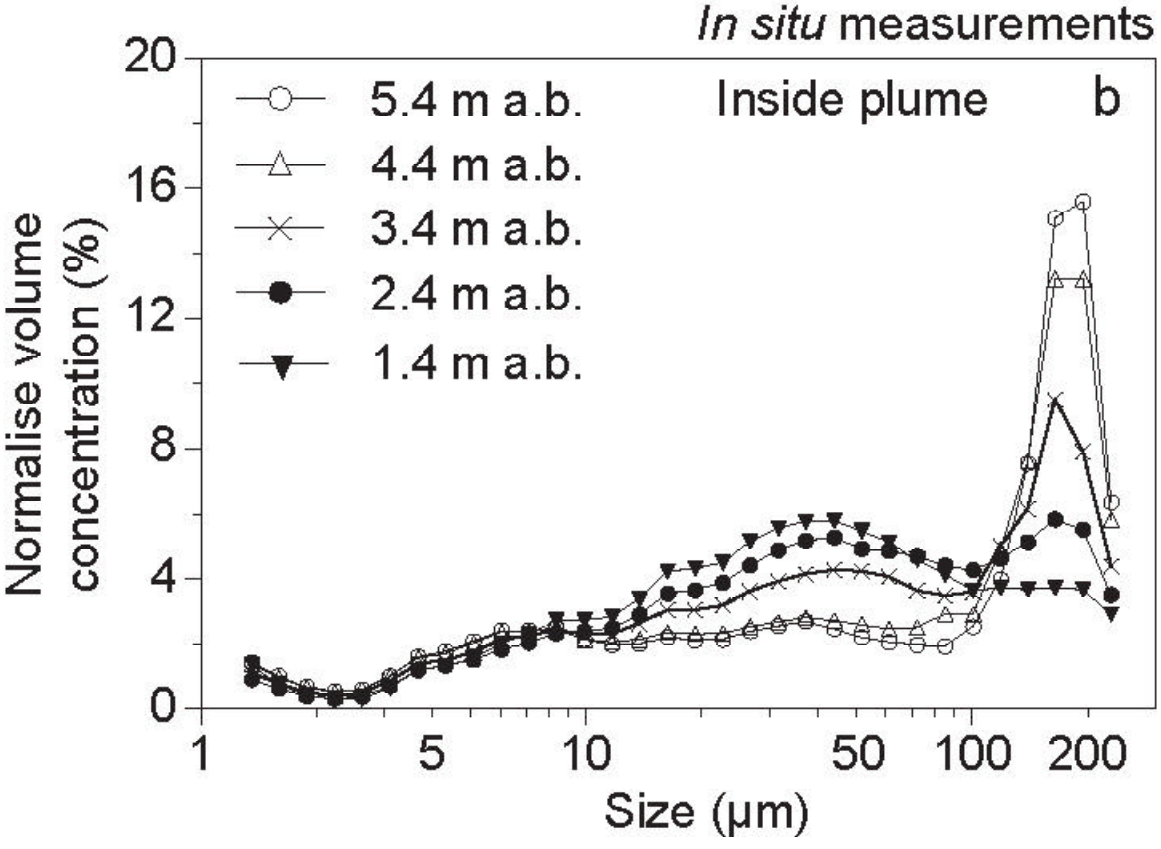
In situ measurements
Inside plume
b
5.4 m a.b.
4.4 m a.b.
3.4 m a.b.
2.4 m a.b.
1.4 m a.b.
Normalise volume concentration (%)
Size (µm)
0
4
8
12
16
20
1
5
10
50
100
200

Figure 10

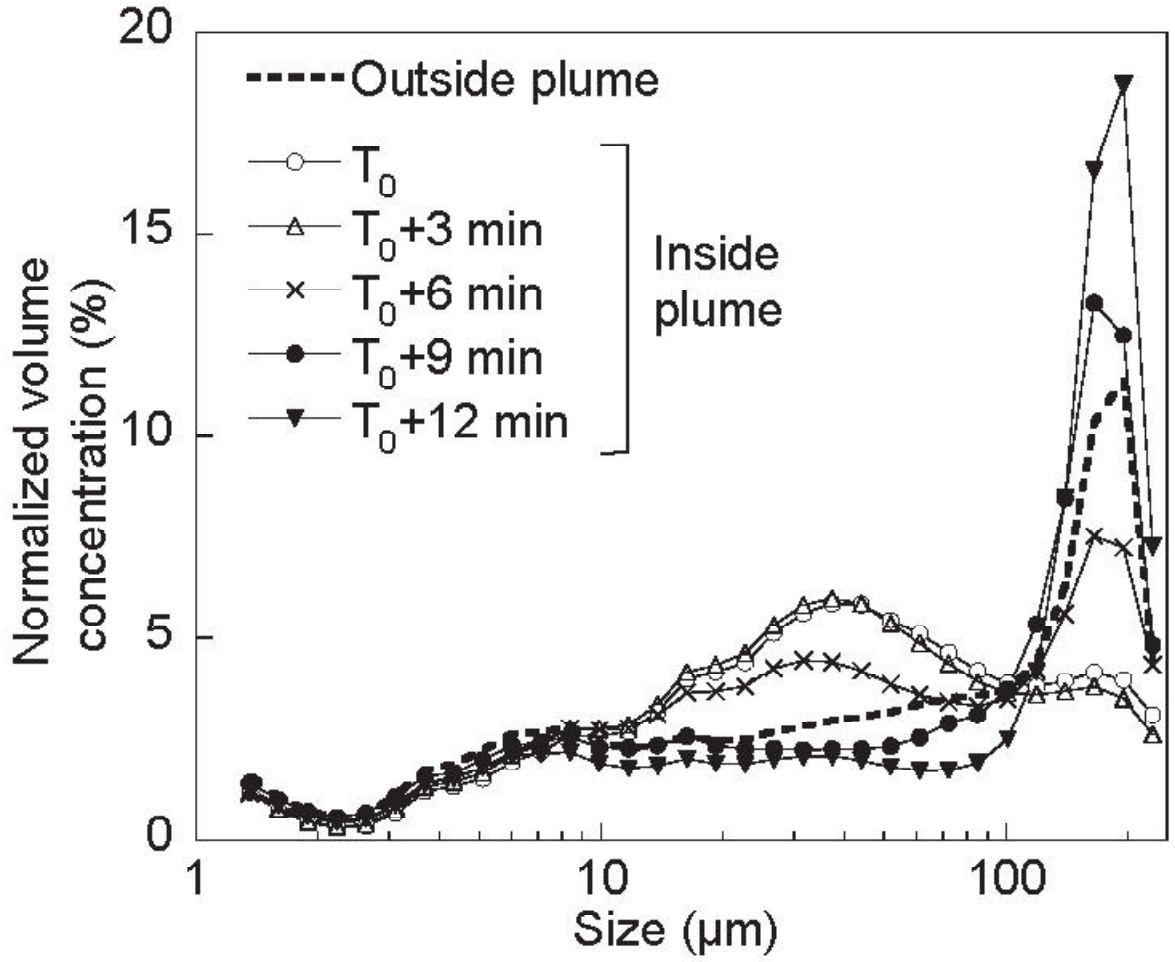
20
15
10
5
0
Normalized volume concentration (%)
Outside plume
T_0
T_0+3 min
T_0+6 min
T_0+9 min
T_0+12 min
Inside plume
1
10
100
Size (μm)

Figure 11

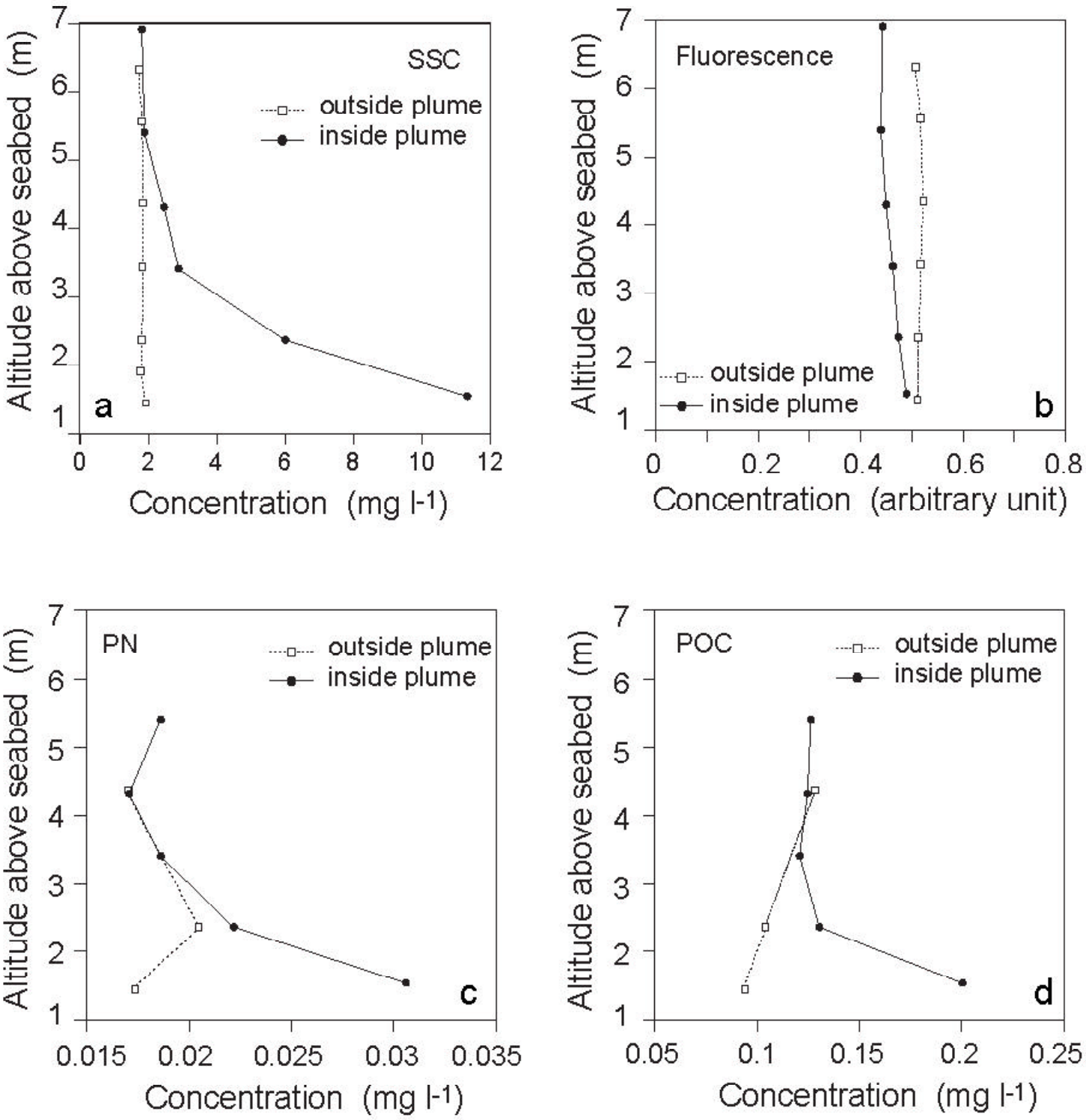
SSC
outside plume
inside plume
a
Altitude above seabed (m)
Concentration (mg l-1)
Fluorescence
outside plume
inside plume
b
Concentration (arbitrary unit)
PN
outside plume
inside plume
c
POC
outside plume
inside plume
d

Figure 12

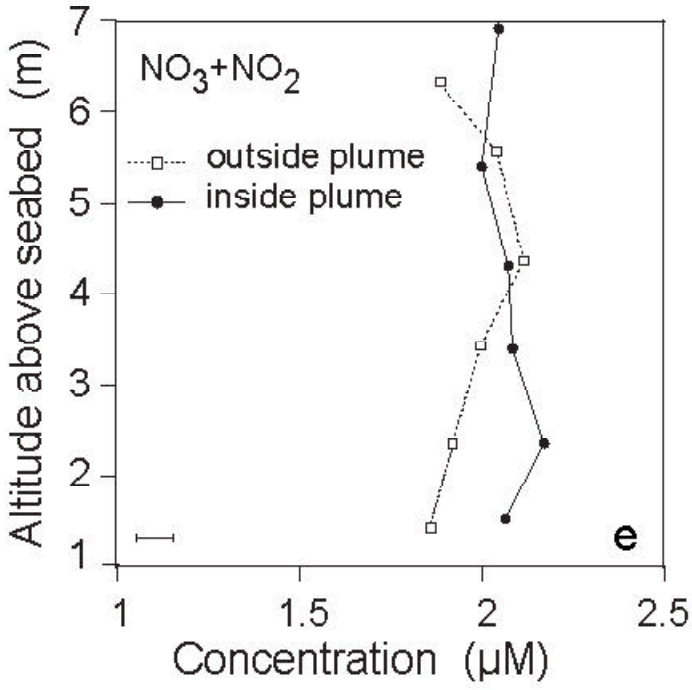

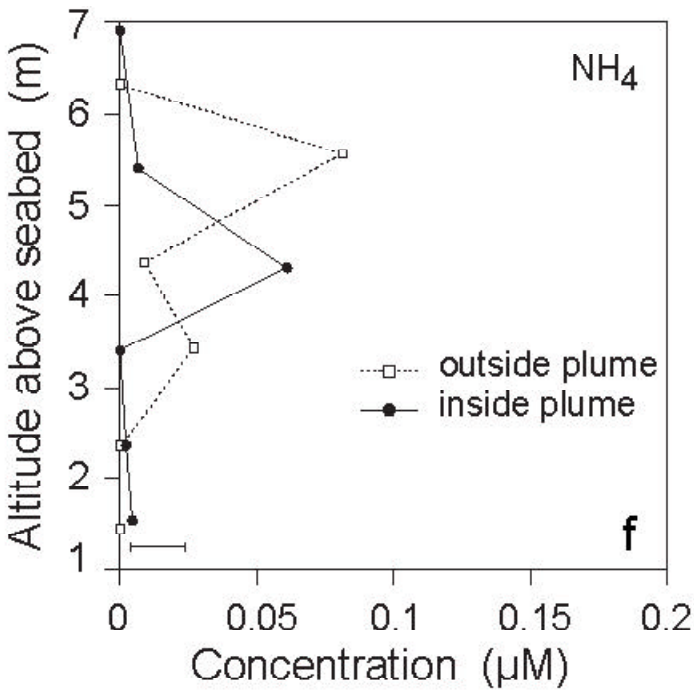

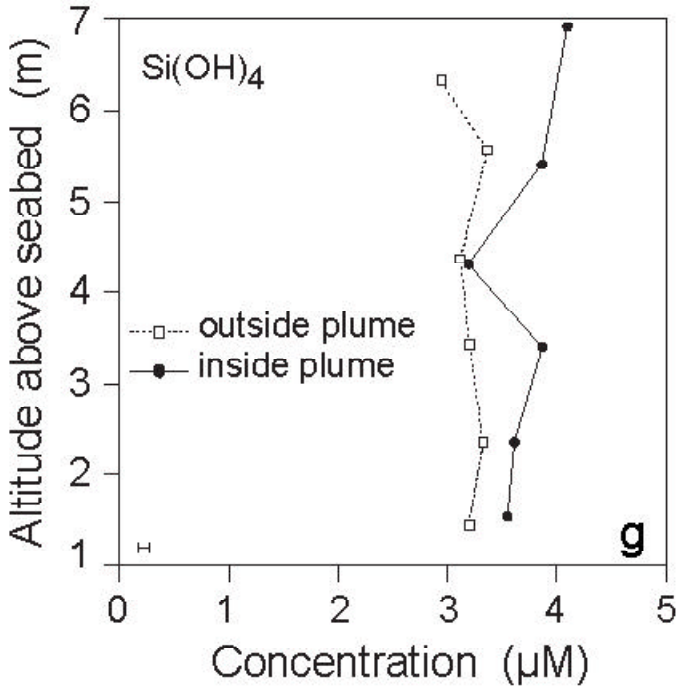

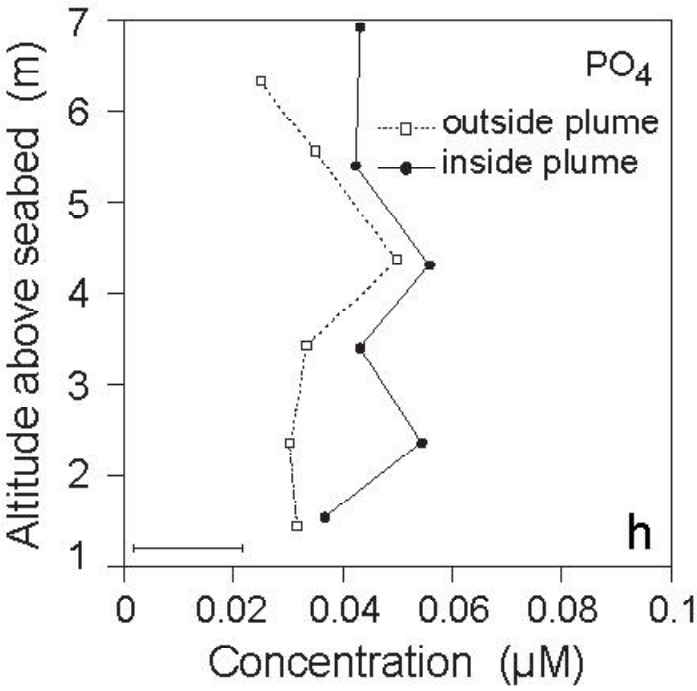

Figure 12 (continued)

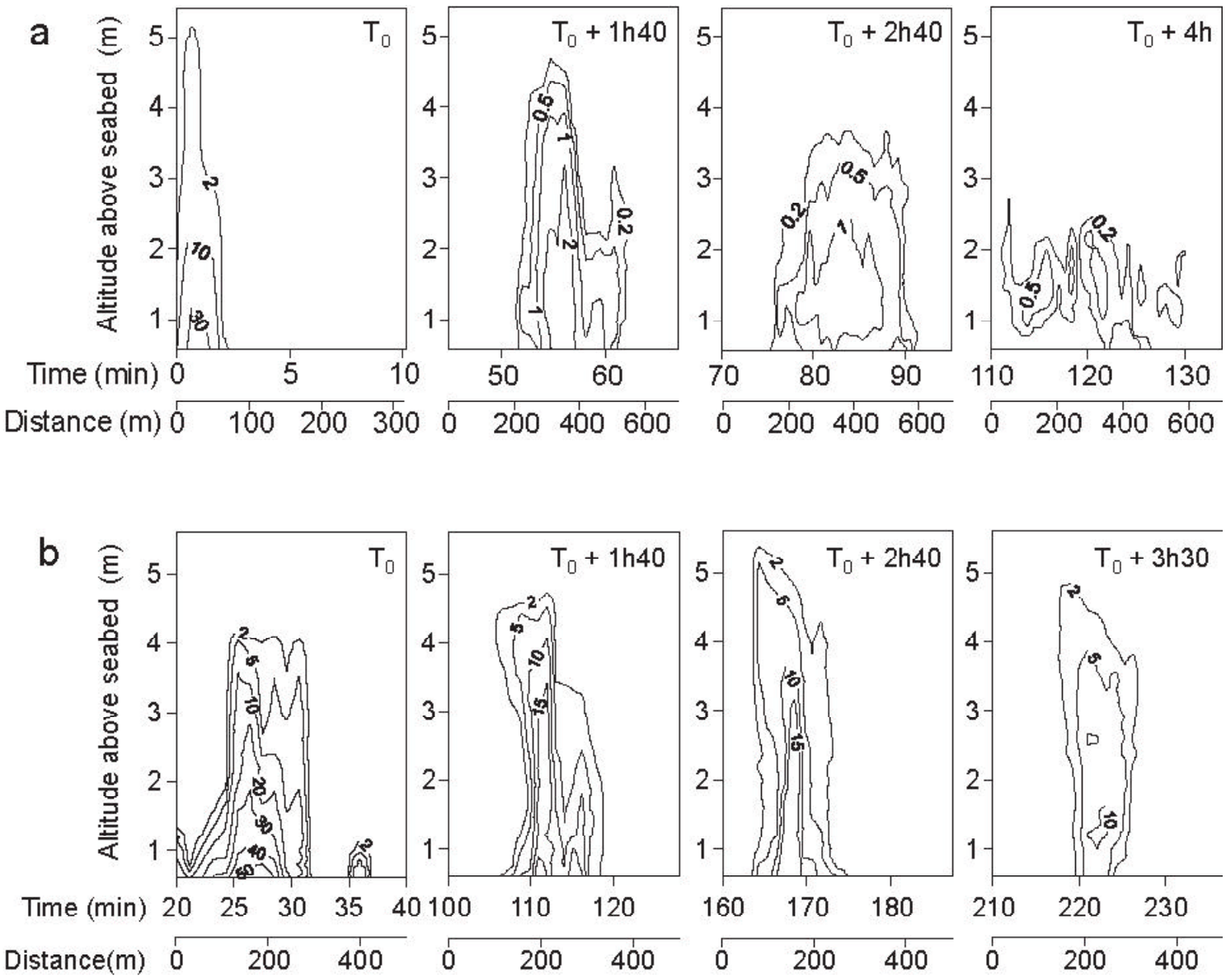
a
Altitude above seabed (m)
T0
T0 + 1h40
T0 + 2h40
T0 + 4h
Time (min)
Distance (m)
b
Altitude above seabed (m)
T0
T0 + 1h40
T0 + 2h40
T0 + 3h30
Time (min)
Distance(m)

Figure 13

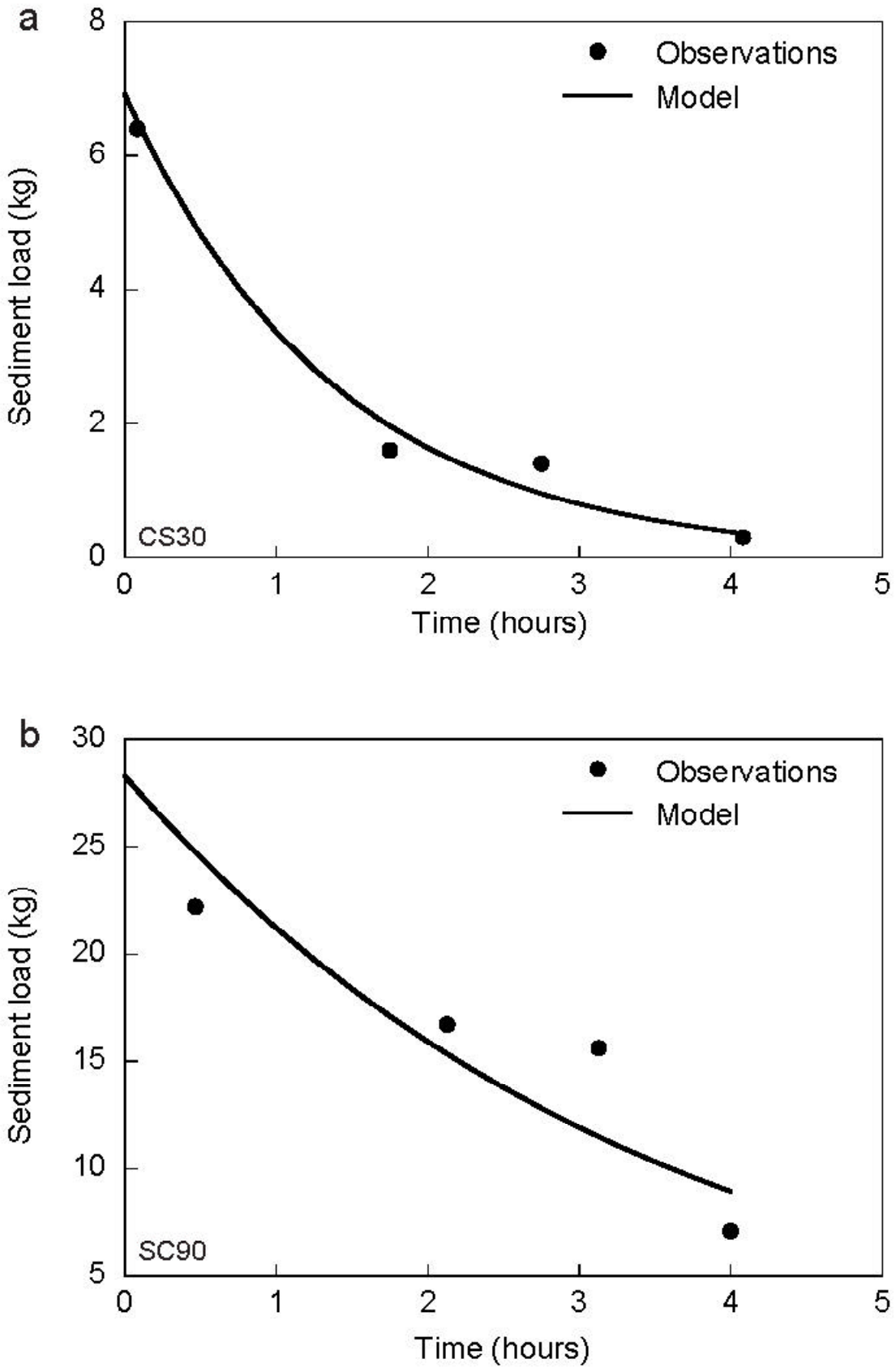
a
Observations
Model
Sediment load (kg)
CS30
Time (hours)
b
Observations
Model
Sediment load (kg)
SC90
Time (hours)

Figure 14